Article:
Cuni-Sanchez, A, Sullivan, MJP, Platts, PJ et al. (99 more authors) (2021) High aboveground carbon stock of African tropical montane forest. Nature, 596. pp. 536-542. ISSN 0028-0836

https://doi.org/10.1038/s41586-021-03728-4

High aboveground carbon stock of African tropical montane forests

Aida Cuni-Sanchez[1,2*], Martin J. P. Sullivan[3,4], Phil Platts[1], Simon L. Lewis[4,5], Rob Marchant[1], Gerard Imani[6], Wannes Hubau[7,8], Iveren Abiem[9,10], Hari Adhikari[11], Tomas Albrecht[12], Janne Altman[12,13], Christian Amani[6], Abreham B. Aneseyee[14,15], Valerio Avitabile[16], Lindsay Banin[17], Rodrigue Batumike[18], Marijn Bauters[19],Hans Beeckman[7], Serge K. Begne[4,20], Amy Bennett[4], Robert Bitariho[21], Pascal Boeckx[19], Jan Bogaert[22], Achim Bräuning[23], Franklin Bulonvu[24], Neil D. Burgess[25], Kim Calders[26], Colin Chapman[27-30], Hazel Chapman[10,31], James Comiskey[32], Thales de Haulleville[33], Mathieu Decuyper[34,35], Ben DeVries[36], Jiri Dolezal [37,38], Vincent Droissart[39], Corneille Ewango[40], Senbeta Feyera[41], Aster Gebrekristos[42], Roy Gereau[43], Martin Gilpin[4], Dismas Hakizimana[44], Jefferson Hall[45], Alan Hamilton[46], Olivier Hardy[47], Terese Hart[48], Janne Heiskanen[11,49], Andreas Hemp[50], Martin Herold[35], Ulrike Hiltner[51,52], David Horak[53], Marie-Noel Kamdem[20], Charles Kayijamahe[54], David Kenfack[45], Mwangi J. Kinyanjui[55], Julia Klein[56], Janvier Lisingo[40], Jon Lovett[4], Mark Lung[57], Jean-Remy Makana[58], Yadvinder Malhi[59], Andrew Marshall [1,60,61], Emanuel H. Martin[62], Edward T.A. Mitchard[63], Alexandra Morel[64], John T. Mukendi [7], Tom Muller[65], Felix Nchu[66], Brigitte Nyirambangutse[67,68], Joseph Okello[19,69,70], Kelvin S.-H. Peh[71,72], Petri Pellikka[11,73], Oliver Phillips[4], Andrew Plumptre[74], Lan Qie[75], Francesco Rovero[76,77], Moses N. Sainge[78], Christine B. Schmitt[79,80], Ondrej Sedlacek[53], Alain S.K. Ngute[60,81], Douglas Sheil[82], Demisse Sheleme[83], Tibebu Y. Simegn[84], Murielle Simo-Droissart[20], Bonaventure Sonké[20], Teshome Soromessa[14], Terry Sunderland[85,86], Miroslav Svoboda[87], Hermann Taedoumg[88,89], James Taplin[90], David Taylor[91], Sean Thomas[92], Jonathan Timberlake[93], Darlington Tuagben[94], Peter Umunay[95], Eustrate Uzabaho[54], Hans Verbeeck[26], Jason Vleminckx[96], Goran Wallin[68], Charlotte Wheeler[63], Simon Willcock[97], John T. Woods [98], Etienne Zibera[67]

Abstract

In the tropics, variation in aboveground live tree biomass carbon (AGC) stocks is poorly understood in montane forests, and especially so for African nations where montane forests often represent most of the extant evergreen old-growth forest cover. Although data are few, since primary productivity is temperature-mediated, and cloud immersion, wind and steep slopes constrain tree height, AGC is widely assumed to be lower in tropical montane than lowland forests. To test this, we assembled and analysed a new dataset ("AfriMont") spanning 44 old-growth montane sites across 12 African countries, and compared findings with old-growth lowland forests in the African Tropical Rainforest Observation Network. We find that montane sites have a mean AGC-stock of 149.4 Mg C ha^{-1} (95% CI 137.1-164.2), higher than montane and lowland forests in the Neotropics and comparable to lowland African forests. Notably, our results are substantially higher than the IPCC default values for these forests in Africa (89.3 Mg C ha^{-1}). The distinctive structure of African lowland tropical forests (low stem density and high abundance of large trees) is mirrored in montane forests. This important carbon store is endangered, 800,000 ha of old-growth montane forest have been lost in the past 18 years in Africa. Our findings highlight the urgent need for the conservation of these biodiversity and carbon-rich forest ecosystems. We provide country-specific estimates to help guide forest conservation and reforestation interventions.

Main text

Tropical forests cover less than 10% of the global land area yet store 40–50% of terrestrial vegetation carbon[1] and contribute more than one third of primary productivity[2] so are a key component of the global carbon cycle[3,4]. There is substantial variation in carbon stocks across the biome, with lowland forests in Africa and Borneo storing more carbon per unit area than lowland forests in the Neotropics[5,6]. This variation arises partly from structural differences: the signature feature of African forests is their low stem density but relatively high abundance of large trees (>70 cm diameter) which store large quantities of carbon, while Bornean forests are characterised by high stem density and basal area[5,7,8].

Despite increased understanding of biogeographic differences in lowland tropical forests, patterns of spatial variation in carbon stocks remain poorly understood in the 880,000 km^2 of montane tropical forests located ≥ 1000 m asl[9]. Montane forests are expected *a priori* to have lower aboveground live tree biomass carbon (AGC) stocks than lowland forests because (1) temperature decreases with increasing elevation, reducing net primary productivity and slowing nutrient recycling, (2) long periods of cloud immersion in montane forests suppresses productivity, (3) soil waterlogging slows nutrient recycling and (4) high epiphyte load, wind exposure and nutrient-limited soils limit tree size and increase investment in roots over shoots[10]. While forest inventory plots provide some support for these assumptions[9] data from African mountain regions are exceptionally sparse. Indeed, in the most recent IPCC guidelines, there is no specific biomass default value for old-growth montane forests in Africa: the value given of 89.3 Mg C ha^{-1} is simply a mean of secondary and old-growth forests found ≥1000 m asl[11]. Mountain areas also pose special challenges for remote sensing approaches for estimating carbon stocks, as radar data are affected by geometric distortions[12] while steep slopes bias spaceborne LiDAR estimates towards overestimating canopy height[13]. These issues are reflected in the lack of correlation between estimates of aboveground carbon stocks from different recent remote sensing derived carbon maps (Table S1).

Better understanding of montane carbon stocks is important for many African countries, particularly in eastern Africa where montane forests represent most of the extant evergreen old-growth forest cover. Quantifying carbon stocks in these ecosystems is critical for estimating national carbon losses from deforestation and forest degradation[14]. Quantifying carbon stocks in old-growth montane forests also clarifies potential carbon uptake by restored natural forests, given the high commitment of most African nations to the Bonn Challenge effort to restore 150 million ha of degraded and deforested lands by 2020 (see Table 1).

Here we compiled, measured and analysed an unprecedented dataset of 226 plot inventories spanning 44 sites in 12 African countries, covering most major mountain regions on the continent (the "AfriMont" dataset). Plots range from 800 to 3900 m asl to include submontane forests in smaller mountains closer to the ocean[15,16]. For all plots, stem diameter and species were recorded for each tree ≥10 cm diameter at breast height (or above buttress) following standard methods[17]. Tree height was sampled in 23 montane sites, allowing variation in height-diameter allometry to be incorporated into the calculation of aboveground biomass. A total of 72,336 stems with diameter ≥10 cm were measured. For each tree, we computed AGC (in Mg C ha^{-1}) according to standard procedures (see methods).

We find that the mean plot-level AGC-stock in tropical montane African forests is 149.4 Mg C ha^{-1} (95% CI 137.1-164.2), two-thirds more than the IPCC default value of 89.3 Mg C ha^{-1}. Our estimates of AGC-stocks in African montane forests are robust to subsampling our dataset (Fig. S1) and excluding small plots (Fig. S2) and are not affected by the sampling strategy used to establish plots in each study site (Fig. S3). Comparing our dataset to previous syntheses of montane[9,18,19] and lowland[6] forest plots reveals that tropical montane forests in Africa have significantly higher AGC-stocks per

unit area than both montane (95% CI = 50.4 – 71.9 Mg C ha^{-1}) and lowland (95% CI = 124.0 – 147.9 Mg C ha^{-1}) forests in the Neotropics, and that they do not differ significantly from lowland forests in Africa (95% CI = -27.6 – 9.6 Mg C ha^{-1}, Fig. 1, Table S2). The similar AGC-stocks in montane and lowland forests in Africa contrasts with the Neotropics and Southeast Asia, where carbon stocks are lower in montane forests than lowland forests (albeit not significantly different in Southeast Asia due to the small sample size, Fig. 1). These differences are robust to accounting for differences in elevation among montane datasets: removing African plots below 1000 m asl slightly reduces estimated AGC-stock to 145.0 Mg C ha^{-1} (95% CI 129.6 – 163.2), but observed differences in AGC-stock among continents remain when plots are restricted to elevations well represented in all continents (Fig. S4).

The characteristic structural properties of lowland African forests (relatively low stem density and greater importance of large trees compared to elsewhere in the tropics[5]) are also evident in African montane forests. In these montane forests mean stem density is 483.3 stems ha^{-1} (± 177.7 SD) and mean basal area is 39 m^2ha^{-1} (± 14.8 SD). We find a high density of large stems (>70 cm diameter, 19.1 stems ha^{-1} ± 15.4 SD) which contribute 35.3% (95% CI = 29.6 – 41.8 %) to plot-level AGC-stock (Fig. 2). The contribution of large trees to plot-level AGC-stock is also similar in montane and lowland Africa (95% CI of difference in square-root transformed proportional contribution of large trees between lowland and montane forests = -0.100 - 0.075, P = 0.80). There was no significant difference in the proportional contribution of any other size class to AGC-stocks between our montane dataset and 132 lowland plots from the AfriTRON network (P≥0.24, Table S3), although greater variation among plots is observed in montane forests (Fig. 2).

To investigate if elevation affected AGC or forest structure, we modelled these variables as functions of elevation using random slopes mixed-effects models. This approach allows intercepts and relationships to vary among sites, which would be expected as mountains can have very different climate at the same elevation due to proximity to the ocean (generally the further, the drier) and because of the mass-elevation or telescopic effect[20] (larger mountains are better at warming the atmosphere above them). We found that AGC, stem density or density of large stems (>70 cm diameter) were not significantly related to elevation (Fig. 3, Table S4). Across sites these non-significant relationships were all negative, although there was some variation in strength and direction amongst sites (Fig. 3). Similarly, in the Neotropics and Southeast Asia montane forest datasets, AGC was not significantly correlated with elevation (Fig. S5).

To assess potential environmental drivers of variation in AGC-stocks in African montane forests, we related them to climate, soil and topography. We found that AGC-stocks increased with annual precipitation (albeit not statistically significantly), decreased with soil fertility and were higher in plots which were locally higher elevation than their surroundings (Fig. S6). Relationships with other environmental variables were non-significant (Fig. S6). Although global datasets might not capture fine-scale variation in climate or soils in mountain regions[21], leading to regression dilution[22], the general absence of strong climate effects combined with the lack of significant effect of elevation on AGC-stocks suggest that the high AGC-stock of African montane forests is a pervasive phenomenon across a wide environmental gradient.

Although the AfriMont dataset covers most major mountain areas in tropical Africa (Fig. 4), some areas are sampled less than expected given the extent of forest there (Fig. S7), resulting in some differences between the environmental conditions sampled by our plot network and the wider biome (Fig. S8). Notably, the absence of plots from the submontane forests of eastern Democratic Republic of the Congo (Fig. 4, Fig. S7) means that the AfriMont dataset samples forests that are on average at higher elevations, cooler and cloudier than the wider biome (Fig. S8). Using relationships with environmental variables (Fig. S6) to predict AGC-stocks in each 1km grid cell containing

montane forest gives a mean (weighted by remaining forest cover) AGC-stock of 176.9 Mg C ha^{-1} for the tropical montane forest biome in Africa, which is higher than the one we report in Fig. 1.

Several mechanisms could explain the unexpectedly high AGC-stock of African montane forests. Firstly, large herbivores such as elephants (*Loxodonta* spp.) can have profound effects on forest structure by consuming biomass, destroying small stems, dispersing seeds and transporting nutrients[23]. Studies for lowland forests suggest that elephants can increase carbon stocks[24,25]. We tested if AfriMont plots with known elephant presence as of 2019 had significantly higher AGC-stocks, but we found that they had significantly lower AGC-stocks, although significant differences were not observed in some countries (Fig. S9). While the initial ecosystem response to elephant removal might be greater AGC-stocks due to reduced biomass consumption and small-stem destruction, the longer-term effects might differ. We were unable to fully disentangle such effects, as we lacked details on both i) time since elephant extirpation, and ii) elephant abundance and its determinants (see Table S5).

A second potential explanation to the high biomass of African montane forests is a relatively low frequency of large-scale abiotic disturbances, allowing trees time to grow large and stands to self-thin, as is seen in lowland African forests[5]. For example, tropical cyclones are rare in mainland Africa (except in Mozambique[26]) and lava flows are rare even in the active volcano of Mt Cameroon[27]. Although fine-scale variability in landslide risk limits comparisons across large spatial scales, there are fewer areas with high landslide susceptibility in mountains in tropical Africa than the Andes and Borneo[28]. If forests have been ecologically stable over evolutionary timescales, tree species may be adapted to grow slowly but potentially reaching great sizes[29]. On Mt Kilimanjaro *Entandrophragma* individuals reach enormous heights and ages[30]. This low frequency of large-scale abiotic disturbances contrasts with the Andes and several mountains in Southeast Asia (e.g. Mt Kinabalu), which are tectonically active, so the trees there are adapted to sudden disturbance followed by intense competition to get established and grow. Future monitoring of the AfriMont plot network will help determine the extent to which the high biomass of African tropical montane forests results from them being dynamic and productive, or adapted to stability.

A third potential explanation could be the presence of conifers[31]. Mixed conifer/broad-leaved forests tend to have greater basal area than purely broad-leaved forests due to a more effective use of light and other resources[32]. Podocarpaceae can be found in montane forests across the tropics[33]. Despite having fewer species in Africa than other continents[34], these could be more abundant at the site-level, but there is no pantropical comparative study on Podocarpaceae abundance in tropical montane forests. In our dataset there was no significant correlation between plot-level AGC-stock and conifer (Podocarpaceae) abundance (Fig. S10). Other explanations could be continental differences in mountain terrain (more gentle slopes or plateau regions in Africa) or types of montane forests investigated (less cloud forest existing/sampled in Africa). Within our dataset, slope did not have a significant effect on AGC-stocks (Fig. S6). Contrary to the Neotropics[35], there is no high-resolution map of cloud forests available for Africa, so while we found no relationship between AGC-stock and cloud frequency (Fig. S6), we were unable to investigate differences in AGC-stock between cloud vs non-cloud plots.

To understand the policy implications of our findings for African countries, we calculated montane (≥800 m asl) forest cover change between 2001 and 2018, using forest cover from ref.[36] clipped to 'primary humid forest' from ref.[37]. We show that tropical montane forests represent most -or all-evergreen old-growth forests found in ten African countries (Fig. 4), and that the Democratic Republic of the Congo has two thirds of the remaining 16 million ha of montane forests in Africa. Over 800,000 ha (5%) have been lost in Africa since 2001, with the highest losses in the Democratic Republic of the Congo (500,000 ha), Uganda (64,000 ha) and Ethiopia (62,000 ha) (Fig. 4, Table 1). In

terms of percentage, Mozambique and Côte d'Ivoire lost over 20% of their montane forests over this period (Fig. 4, Table 1). In some sites, however, a larger proportion of montane forests was lost before 2001, e.g. in Taita Hills in Kenya[38]. If absolute country-level deforestation rates are to continue, another 0.5 million hectares of tropical montane forests will be lost by 2030.

African tropical montane forests are not only carbon-rich, but they also harbour some of the highest concentrations of biodiversity and endemism in the world [39,40]. They are important water towers as, located at the headwaters of numerous river systems, they regulate timing and magnitude of runoff[39]. They also regulate local temperatures[41] and provide numerous other services to people in the surrounding landscapes[39]. Clearly, more should be done to avoid the destruction of these important ecosystems. Logging, mining and clearing land for farming, but also political unrest and militia presence have affected -and continue to affect- these forests, e.g. in Itombwe Mts in Democratic Republic of the Congo[42]. Protected areas are known to help reduce deforestation in the tropics[43]. Beyond protected areas, other forest conservation mechanisms could be implemented, including effective carbon finance. Previous IPCC AGC-stock estimates for montane forests in Africa (89.3 Mg C ha^{-1}) may have contributed to low incentives for carbon finance mechanisms in these ecosystems. Our study shows the far greater carbon storage potential in these tropical montane forests, which will be even higher if soil carbon stocks are considered (e.g. > 200 Mg C ha^{-1} of organic carbon occurs in the top 0-30 cm soil on Mt Cameroon[44] or the Usambara Mountains[45]).

As well as conserving the remaining montane forests, efforts to restore them are critical. Forest restoration at one of our sites, Kibale National Park in Uganda, indicates the potential for rapid AGC accumulation[46]. Our study shows the high potential AGC-stock these forests can attain. The possible co-benefits of forest restoration, notably water regulation, control of soil erosion and landslides and biodiversity conservation should also be considered. Most African nations are committed to the Bonn Challenge; Ethiopia leading with 15 million ha committed (Table 1). We provide country-specific estimates of potential AGC-stocks (Table 1, Fig. S11) to help guide such interventions. Caution is needed when scaling-up our estimates to the landscape scale, as not all forests are closed-canopy old-growth and structurally intact. Remote sensing or ancillary data (landcover maps, spatial environmental data) could be used to identify e.g. exotic plantations, degraded or bamboo forests, and help create a detailed AGC map at different spatial scales[14,46].

Our newly compiled dataset and analysis has provided the first large-scale quantification of AGC-stock in montane tropical Africa, and demonstrated it to be high on average. While there is variation around this AGC-stock mean within and across sites, it is not systematically related to elevation. Apart from helping refine country-level estimates, revise IPCC guidelines and help calibrate remote sensing estimates, continued on-the-ground monitoring of the AfriMont plot network will help determine forest dynamics and carbon residence time of these extraordinarily carbon-rich forests, as well as their responses to climatic changes.

Figures main document

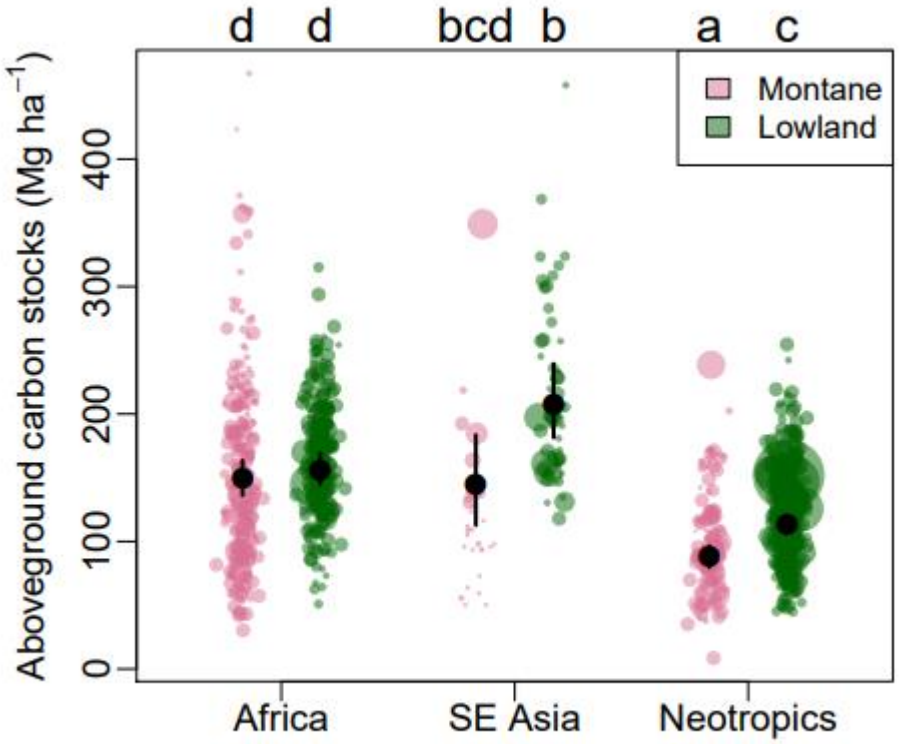

Fig. 1. Pantropical variation in aboveground carbon stocks in montane (>800 m asl) and lowland (< 800 m asl) tropical forests. Data from this study for African montane forests (n = 226 plots), montane forests in the Neotropics (n = 131) and Southeast Asia (n = 32) from ref.[9,16,17] , lowland forests in Africa (n = 290), the Neotropics (n = 416) and Southeast Asia (n = 60) from ref.[6]. Coloured points show the AGC-stock in each plot, with point size proportional to square-root plot area. Black points show means for each continent-elevation category estimated using linear mixed effects models with site as a random effect, and lines show 95% confidence intervals around means. Letters indicate signficiant differences between continent elevation category combinations (linear mixed-effects models with site as a random effect, $P < 0.05$).

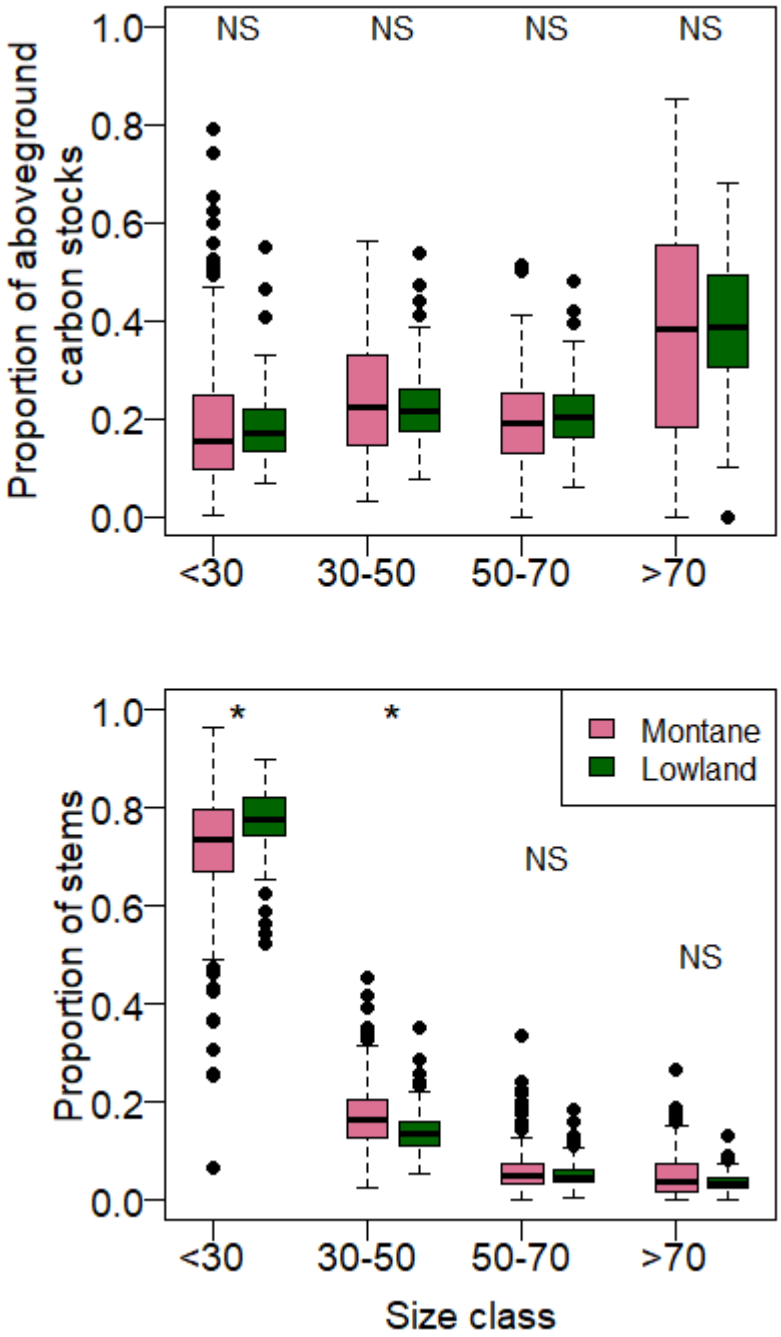

Fig. 2. Proportion of plot-level aboveground carbon stock (top) and stems (bottom) accounted for by each size class (in cm) in montane (n =226) and in lowland (n =132) forests in Africa. Statistically significant differences in contribution of each size class between montane and lowland forests are shown by asterisks (linear mixed-effects model, $P < 0.05$). NS = non-significant difference.

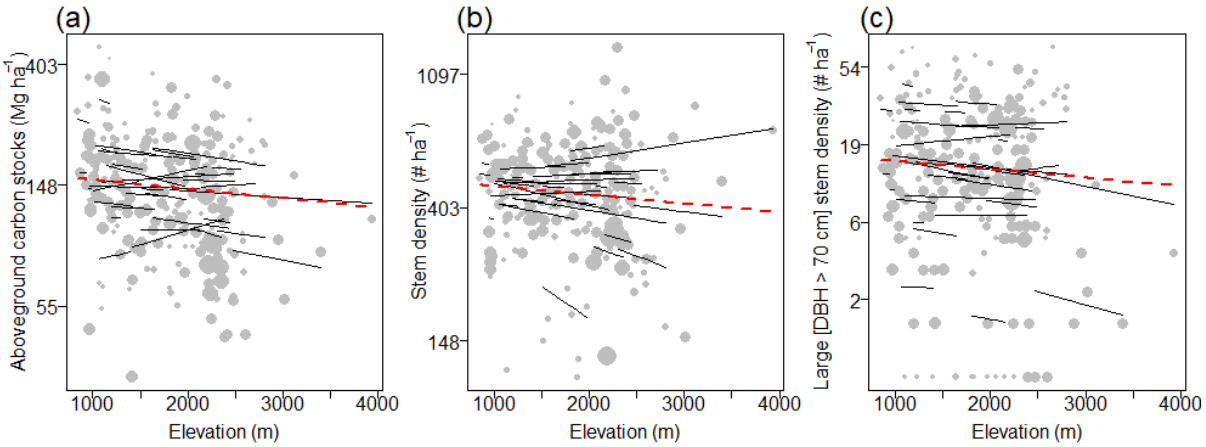

Fig. 3. Relationship between elevation and (a) plot-level aboveground carbon stock, (b) stem density and (c) stem density of large stems (>70 cm diameter) for the AfriMont dataset. Each response variable was log-transformed and modelled as a function of elevation with a linear mixed-effect models with random slopes. The dashed red line shows the relationship across sites (non-significant in all cases, $P \geq 0.3$, Table S3), while the black lines show the relationship within each site. Point sizes are proportional to square-root plot area. A polynomial model allowing a non-linear relationship with elevation was also tested but not supported over the linear model in any case ($P \geq 0.7$, Table S3). The absence of a significant relationship with elevation is robust to removing the two highest elevation sites, RWE and VIR (Table S4).

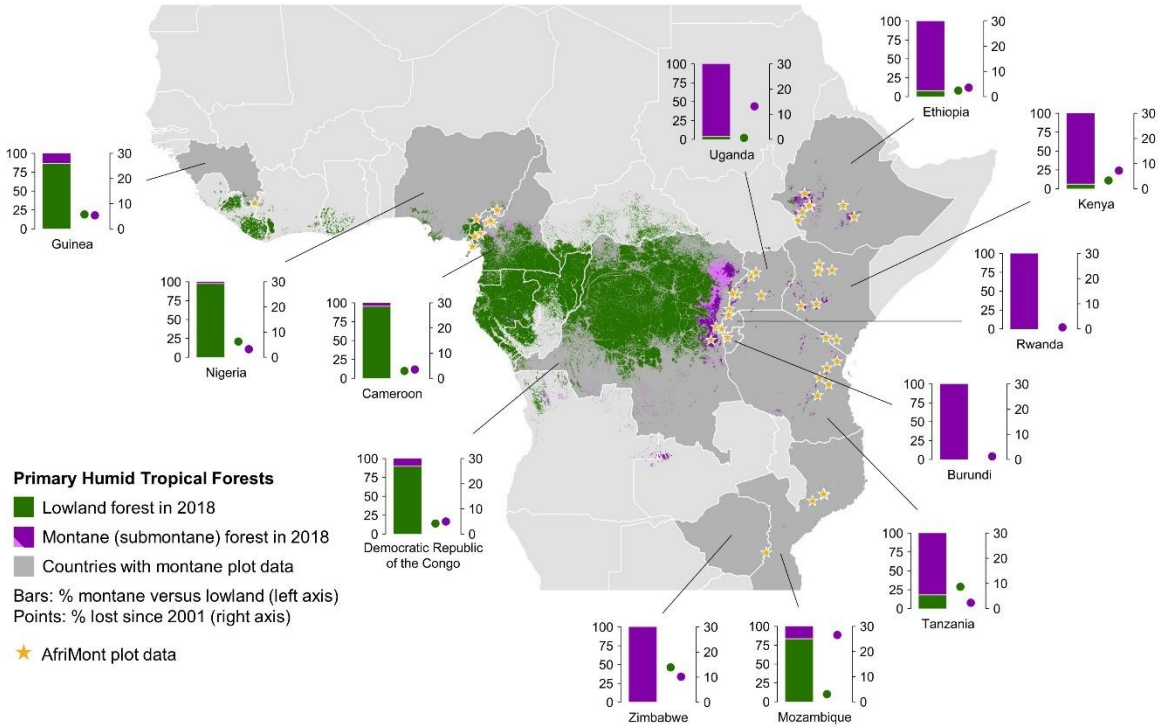

Fig. 4. Old-growth evergreen humid forests in lowland and montane tropical Africa as per December 2018. Note that montane includes submontane forests (800-1000 m asl, light purple) and that countries have different y-axis. Montane forests represent most (or all) evergreen humid old-growth forests found in ten African nations: Burundi, Ethiopia, Kenya, Rwanda, Tanzania, Uganda and Zimbabwe (included in AfriMont); and Zambia, Malawi and South Sudan (no plot data available). Forest cover extracted from ref.[33], clipped to 'primary humid forest' using ref.[34]. See Table 1 for country-level absolute estimates.

Table 1 For each country studied, commitment to the Bonn Challenge, surface of remaining old-growth montane forest area (as per December 2018), montane forest lost for the period 2001-2018, modelled mean aboveground carbon (AGC, in Mg C ha^{-1}) estimates for montane forests, and number of sites and plots used for these AGC estimates. For comparison at the country level, surface, mean AGC and number plots used for AGC estimates for lowland forests are also provided.

Country	Bonn Challenge (ha)	Montane (ha)	Montane lost (ha)	Montane AGC	Montane sites (plots)	Lowland (ha)	Lowland AGC	Lowland plots
Burundi	2 million	25,000	308	94 (47-176)	1 (7)	0		0
Cameroon	12 million	845,000	30,469	153 (121-195)	7 (37)	17.7 million	166 (151-185)	72
DRC	8 million	10.2 million	537,722	129 (84-202)	2 (37)	90 million	158 (135-183)	48
Ethiopia	15 million	1.7 million	62,607	165 (124-215)	8 (25)	146,000	[a]	0
Guinea	2 million	30,000	1,682	314 (147-616)*	1 (2)	196,000	157 (122 – 206)[c]	24
Kenya	5.1 million	569,000	44,219	104 (79-136)	8 (38)	37,000		0
Mozambique	1 million	19,000	6,943**	226 (146-384)*	3 (4)	98,000	[b]	0
Nigeria	4 million	42,000	1,380	120 (47-309)*	1 (1)	1.7 million	161 (105-262)	2
Rwanda	2 million	54,000	328	106 (65-168)	2 (11)	0		0
Tanzania	5.2 million	591,000	14,049	175 (129-234)	6 (29)	131,000	128 (101-163)	16
Uganda	2.5 million	427,000	64,642**	158 (111-209)	6 (23)	18,000		0
Zimbabwe	2 million	7,000	815**	203 (108-363)	1 (12)	<1,000		0

[a] ref. 48 report 192 Mg C ha^{-1} for lowland; [b] ref. 49 report 132.2 Mg C ha^{-1} for lowland . [c] Data from neighbouring Liberia.
* few plots sampled, or very small plots sampled, AGC estimates may not be robust, see Fig. S8 in Supplementary Material.
**Montane forest loss in Mozambique, Uganda and Zimbabwe represents 27%, 13% and 10% of the existing montane forest in 2001, respectively. Montane forest loss in Côte d'Ivoire (no plot data available) was estimated to be 21% for the same period.

References

1. Erb, K., et al. Unexpectedly large impact of forest management and grazing on global vegetation biomass. *Nature* **553**, 73–76 (2018).
2. Pan, Y. et al. A large and persistent carbon sink in the world's forests. *Science* **333**, 988–993 (2011).
3. Booth, B. B. B. et al. High sensitivity of future global warming to land carbon cycle processes. *Environ. Res. Lett.* **7**, 024002 (2012).
4. Hubau, W., et al. Asynchronous carbon sink saturation in African and Amazonian tropical forests. *Nature* **579**, 80–87 (2020).
5. Lewis, S. L. et al. Above-ground biomass and structure of 260 African tropical forests. *Phil. Trans. R. Soc. Lond. B* **368**, 20120295 (2013).
6. Sullivan, M. J. P., et al. Long-term thermal sensitivity of Earth's tropical forests. *Science* **368**, 869–874 (2020).
7. Feldpausch, T. R. et al. Tree height integrated into pantropical forest biomass estimates. *Biogeosciences* **9**, 3381–3403 (2012).
8. Bastin, J.-F., et al. Pan-tropical prediction of forest structure from the largest trees. *Global Ecol. Biogeogr.* **27**, 1366–1383 (2018).
9. Spracklen, D.V. & Righelato, R. Tropical montane forests are a larger than expected global carbon store. *Biogeosciences* **11**, 2741-2754 (2014).
10. Fahey, T. J., Sherman, R. E. & Tanne, E. V. J. Tropical montane cloud forest: environmental drivers of vegetation structure and ecosystem function. *J. Trop. Ecol.* **32**, 355–367 (2016).
11. IPCC. Chapter 4: Forest land. In: D. Blain, F. Agus, M. A. Alfaro & H. Vreuls (Eds.), 2019 Refinement to the 2006 IPCC Guidelines for National Greenhouse Gas Inventories. (Vol. 4): Agriculture, Forestry and Other Land Use (p. 68)(2019).
12. CCI BIOMASS Product User Guide Year 1 Version 1.0. (2019) https://climate.esa.int/sites/default/files/biomass_D4.3_Product_User_Guide_V1.0.pdf
13. Lefsky, M. A., Keller, M., Pang, Y., de Camargo, P. & Hunter, M. O. Revised method for forest canopy height estimation from the Geoscience Laser Altimeter System waveforms. J. *Appl. Remote Sens.* **1**, 013537 (2007).
14. Willcock, S., et al. Quantifying and understanding carbon storage and sequestration within the Eastern Arc Mountains of Tanzania, a tropical biodiversity hotspot. *Carbon Balance Manage.* **9**, 2 (2014).
15. Bussmann, R.W. Vegetation zonation and nomenclature of African Mountains – An overview. *Lyonia* **11**, 41–66 (2006).
16. Hamilton, A. Vegetation, climate and soil, altitudinal relationships on the East Usambara Mountains of Tanzania. *J. E. Afr. Nat. Hist.* **87**, 1-5 (1998).
17. Phillips, O., Baker, T., Brienen, R. & Feldpausch, T. RAINFOR field manual for plot establishment and remeasurement. http://www.rainfor.org/upload/ManualsEnglish/RAINFOR_field_manual_version_2016.pdf (Univ. Leeds, 2016).
18. Vilanova, E. et al. Environmental drivers of forest structure and stem turnover across Venezuelan tropical forests. *PLoS ONE* **13**(6): e0198489 (2018).
19. Alvarez-Davila, E. et al. Forest biomass density across large climate gradients in northern South America is related to water availability but not with temperature. *PLoS ONE* **12**(3): e0171072 (2017).
20. Jarvis, A. & Mulligan, M., The climate of cloud forests. *Hydrol. Process.* **25**, 327–343 (2011).
21. Platts, P.J., Omeny, P.A. & Marchant, R. AFRICLIM: high-resolution climate projections for ecological applications in Africa. *Afr. J. Ecol.* **53**, 103–108 (2015).
22. McInerny, G. J., Purves, D. W. Fine-scale environmental variation in species distribution modelling: Regression dilution, latent variables and neighbourly advice. *Methods Ecol. Evol.* **2**, 248–257 (2011).

23. Poulsen, J.R., et al. Ecological consequences of forest elephant declines for Afrotropical forests. *Conserv. Biol.* **32**, 559–567 (2018).
24. Berzaghi, F., et al. Carbon stocks in central African forests enhanced by elephant disturbance. *Nat. Geosci.* **12**, 725–729 (2019).
25. Enquist, B.J., et al. The megabiota are disproportionately important for biosphere functioning. *Nat. Commun.* **11**, 699 (2020).
26. Lin, T.-C., Hogan, J.A. & Chang, C.T. Tropical Cyclone Ecology: A Scale-Link Perspective. *Trends Ecol. Evol.* **35**, 594–604 (2020).
27. Favalli, M., et al. Lava flow hazard and risk at Mt. Cameroon volcano. *Bull. Volcanol.* **74**, 423–439 (2012).
28. Stanley, T. & Kirschbaum, D.B. A heuristic approach to global landslide susceptibility mapping. *Nat. Hazards* **87**, 145–164 (2017).
29. Lovett, J. C. Elevational and latitudinal changes in tree associations and diversity in the Eastern Arc mountains of Tanzania. *J. Trop. Ecol.* **12**, 629–650 (1996).
30. Hemp, A., et al. Africa's highest mountain harbours Africa's tallest trees. *Biodiv. Conserv.* **26**, 103–113 (2016).
31. Culmsee, H., Leuschner, C., Moser, G. & Pitopang, R., Forest aboveground biomass along an elevational transect in Sulawesi, Indonesia, and the role of Fagaceae in tropical montane rain forests. *J. Biogeogr.* **37**, 960–974 (2010).
32. Enright, N.J. & Ogden, J. The southern conifers - a synthesis. Ecology of the southern conifers (ed. by N.J. Enright & Hill R.S.), pp. 271–287. Melbourne University Press, Melbourne (1995).
33. Neale, D. B. & Wheeler, N. C. The Conifers. In: The Conifers: Genomes, Variation and Evolution (eds. Neale, D. B. & Wheeler, N. C.) pp 1–21. Springer International Publishing (2019).
34. Mill, R. R. Towards a Biogeography of the Podocarpaceae. In IV International Conifer Conference, R. R. Mill, ed. *Acta Hort.* **615**, 137–147 (2003).
35. Helmer, E.H., Gerson, E.A., Baggett, L.S., Bird, B.J., Ruzycki, T.S. & Voggesser, S.M. Neotropical cloud forests and paramo to contract and dry from declines in cloud immersion and frost. PLoS ONE **14**(4): e0213155 (2019).
36. Hansen, M. C., et al. High-Resolution Global Maps of 21st-Century Forest Cover Change. *Science* **342**, 850-853 (2013).
37. Turubanova, S., Potapov, P., Tyukavina, A. & Hansen M. Ongoing primary forest loss in Brazil, Democratic Republic of the Congo, and Indonesia. *Environ. Res. Lett.* **13**, 074028 (2018).
38. Pellikka, P. K. E., Lötjönen, M., Siljander, M. & Lens, L. Airborne remote sensing of spatiotemporal change (1955–2004) in indigenous and exotic forest cover in the Taita Hills, Kenya. *Int. J. Appl. Earth Obs.* **11**, 221–232 (2009).
39. United Nations Environment Programme (UNEP) African Mountains Atlas. UNEP, Nairobi, Kenya (2014).
40. Rahbek, C., et al. Humboldt's enigma: What causes global patterns of mountain biodiversity? *Science* **365**, 1108–1113 (2019).
41. Zeng, Z. et al. Deforestation-induced warming over tropical mountain regions regulated by elevation. *Nat. Geosci.* (2020). https://doi.org/10.1038/s41561-020-00666-0
42. Spira, C., Kirkby, A., Kujirakwinja, D. & Plumptre, A. J. The socio-economics of artisanal mining and bushmeat hunting around protected areas: Kahuzi– Biega National Park and Itombwe nature reserve, eastern Democratic Republic of Congo. *Oryx* **53**, 136–144(2017).
43. Bebber, D.P. & Butt, N. Tropical protected areas reduced deforestation carbon emissions by one third from 2000-2012. *Sci. Rep.* **7**, 14005 (2017).
44. Tegha , K. C. & Sendze, Y. G., Soil organic carbon stocks in Mt Cameroon National Park under different land uses. *J. Ecol. Nat. Environ.* **8**, 20–30, (2016).

45. Munishi, P.K.T. & Shear, T.H. Carbon storage in afromontane rain forests of the eastern arc mountains of Tanzania: their net contribution to atmospheric carbon. *J. Trop. For. Sci.* **16**, 78–98 (2004).
46. Wheeler, C.E., et al. Carbon sequestration and biodiversity following 18 years of active tropical forest restoration. *Forest Ecol. Manage.* **373**, 44–55 (2016).
47. Avitabile, V., Baccini, A., Friedl, M.A. & Schmullius, C. Capabilities and limitations of Landsat and land cover data for aboveground woody biomass estimation of Uganda. *Remote Sens. Environ.* **117**, 366–380 (2012).
48. Aneseyee, B A., Soromessa, T. & Belliethathan, S. Carbon Sock of Gambella National Park: Implication for Climate Change Mitigation. *Int. J. Adv. Life Sci.* **35**, 41–56 (2015).
49. Lisboa, S.N., et al. Biomass allometric equation and expansion factor for a mountain moist evergreen forest in Mozambique. *Carbon Balance Manage.* **13**, 23 (2018).

Methods

AfriMont -montane Africa dataset

We compiled forest inventory plot data from the African Tropical Rainforest Observatory Network (AfriTRON; www.afritron.org), with data curated at www.ForestPlots.net[50,51], and the TEAM network[52], as well as from numerous site-specific publications detailed in Table S5 and mapped in Fig. 4. Plots were selected for the analysis when conforming to the following criteria: ≥800 m asl, closed-canopy evergreen wet or moist tropical forest, geo-referenced, old-growth and structurally intact (not impacted by recent selective logging, fire or coffee cultivation), with no exotic species present (e.g. *Eucalyptus* or *Pinus* spp.), all trees ≥10 cm diameter measured and majority of stems identified to species. We included plots from Virunga Massif in Rwanda/Uganda even if these were not 100% closed-canopy due to high abundance of naturally-occurring bamboo. In all plots, tree diameter was measured at 1.3 m along the stem from the ground, or above buttresses if present. In 23 sites tree height was sampled in the field for some stems, using a clinometer or a laser. Families and species names follow the African Plant Database (ville-ge.ch/cjb/bd/africa/). The AfriMont dataset consists of 72,336 stems, of which 92.9% were identified to species, 98.4% to genus and 98.5% to family. This dataset represents a standardised safe long-term repository of valuable historical data (four sites initially considered could not be included because tree-level data had already been lost by data owners).

AfriTRON -lowland Africa dataset

The 132 lowland-forest plots are all from AfriTRON[4,5,53]. They were selected using the same criteria as above (but with elevation <800 m asl), restricted to countries for which we also had montane plots plus neighbouring countries where the mountains span international borders (e.g. Mt Nimba spans Guinea and Liberia). The dataset includes 51,305 stems, of which 89.6% were identified to species, 97.3% to genus and 97.7 % to family. The plot data was retrieved from forestplot.net on 06/01/2019. The plot locations and details are in Table S6.

Literature dataset

We compiled data on AGC-stocks in lowland and montane forests to compare to the AfriMont data. Data for lowland forests came from ref.[6], and consisted of all multi- and single-census plots that were <800 m asl. Data for montane forests were obtained from ref. [9], with additional data from Venezuela (ref.[18]) and Colombia (ref.[19]). Montane plots were defined as >800 m asl; elevation was not provided for the Colombian dataset so plots were

selected based on the forest type, and these plots were not included in analyses requiring elevation. To avoid double counting plots, Venezuelan and Colombian plots were removed from the ref. [9] dataset.

Aboveground carbon

For each tree in the montane dataset we used the published allometric equation by ref.[54] to estimate aboveground biomass. This allometric equation was created using data from directly harvested trees at 58 sites across the tropics, including eight sites with elevation >800m asl (range 900-3,000m asl including sites in Africa). We then converted this biomass to carbon, assuming that aboveground carbon (AGC, in Mg C ha^{-1}) is 45.6% of aboveground biomass[55]. AGC for each plot was estimated as the sum of the AGC of each living stem, divided by planimetric plot area (in hectares). If field measurements of slope were unavailable, we converted surface to planimetric area extracting slope from the SRTM product. We excluded tree ferns, bamboo and palms, as these were not measured in all plots. Ref.[54] includes tree diameter, wood mass density and tree height. The best taxonomic match wood density of each stem was extracted from a global database[56,57] following ref.[53]. For some sites, all trees in a plot had been sampled for height. If this was not the case, but some field measurements of height were available (typically ten stems per diameter class), we constructed a site-specific height-diameter model, using a Weibull equation[58]. If no field measurements of height were available, we constructed a cluster-specific height-diameter model, using a Weibull equation, as explained in Table S6 in Supplementary Information. The same approach was used to calculate aboveground biomass for lowland forests. For these, height was estimated using regional using a Weibull equation[58].

Small plots and data subsampling

For 22 sites where plots were small (<0.2 ha), we aggregated plots to groups of about 0.2 ha based on their geographic proximity, elevation, environmental affinity and the co-authors' knowledge of the site, to help reduce the variation among plots at site level. This is because the presence of an extremely large tree in a small plot can result in overestimates of AGC[59]. We investigated if using the aggregated-plot approach affected AGC-stock estimates at the site level, and this was not the case (see Fig. S2). We also investigated if including small plots affected the continental mean AGC-stock estimates, as small plots have greater edge surface, and there is a tendency of some field teams to include large trees inside plots when laying out the boundaries[60]. Including small plots did not significantly affect our continental mean AGC-stock estimates (see Fig. S2). We also explored the sensitivity of our continental mean AGC-stock estimates to data subsampling. Data were resampled at different sample sizes either at plot level (sampling with replacement) or at site level (sampling without replacement). The number of plots (n=226) and the number of sites (n=44) we sampled indicate that our estimates of AGC-stock at the continental level are robust (see Fig. S1). They are also not affected by the fact that we included plots 800-1000 m asl (see Fig. S4).

Size classes

For all plots, we computed the proportion of AGC which was distributed in each size-diameter class, using the classes of ref.[8]. We also computed stem density, basal area, density of large trees (>70 cm diameter, named SD_{70} in stems ha^{-1}) and Podocarpaceae abundance (in percentage of plot-level basal area).

Environmental variables and their effects

Climate variables (temperature annual mean and seasonality, and precipitation mean and seasonality, i.e. Bio1, 4, 12 and 15) were extracted from WorldClimV2[61] at 30 arc-sec (~1 km) resolution. Mean temperature values were adjusted for the difference in elevation between the plot and the wider 1 km grid-cell using the lapse rate of -0.005°C m^{-1}. We obtained data on cloud cover from ref.[62] and lightning frequency (0.1 degree, ~11 km) from the LIS very high resolution climatology[63]. Values for soil variables (cation exchange capacity, CEC, representing soil fertility, and percentage clay representing soil texture) were extracted from SoilGrids[64] (~ 1km resolution) and a depth-weighted mean taken for values from 0 to 30 cm depth to give a single value of each soil variable per plot. Elevation was obtained from SRTM (at 3 arc second resolution, ~ 90 m). Topography metrics were calculated from elevation data using the terrain function in the raster R package. These were slope and topographic position index (TPI). TPI is the difference between the elevation of the plot and the mean value of the eight surrounding grid cells – positive values indicate locally high locations and negative values indicate locally low locations. Where small plots were aggregated for analysis, environmental variables were extracted for the ungrouped plot locations, and then an area-weighted mean taken to obtain a plot-level value.

Elephant and conifer effects on AGC-stocks

For the current elephant presence in the AfriMont plots, we created a binary variable (presence/absence) based on co-authors knowledge of elephant ranges and elevation distribution at each site as of 2019. Co-authors estimated that elephants were present in 2019 in 54 plots in 12 sites in five countries (see Table S5). For all plots which had at least one individual of Podocarpaceae family (47 plots, 16 sites, 7 countries), we computed the contribution of Podocarpaceae to plot basal area and AGC-stock in terms of percentages.

Estimating forest cover and loss

We obtained estimates of forest cover and loss in the years 2001 through to 2018, using the 'loss year' dataset of the Global Forest Change database, version 1.6 (ref.[36]). To exclude plantation forests, 'dry' forests (e.g. miombo woodland) and degraded forests, we applied the 'primary humid forest' mask developed by ref.[37]. We distinguished montane from lowland forests using an elevational cut-off of 800-m elevation, using the SRTM v3 product at 1 arc-sec resolution (snapping to the ref.[36] grid of the same resolution). Where there were gaps in the 1 arc-sec SRTM product, we filled these using a 1 arc-sec bilinear interpolation of the (gapless) 3 arc-sec SRTM product. To estimate future forest loss by year 2030, we extrapolated absolute country-level deforestation rates for the period 2001-2018 (in ha per year).

Investigating AfriMont representativeness

To quantify AfriMont sampling effort within the biome, we used the map of tropical montane forest extent (see above) and calculated the amount of remaining forest in each 1-degree grid-cell. By dividing the area sampled by the AfriMont dataset by the proportion of the biome in a grid-cell, we calculated the expected sampling intensity if sampling was proportional to remaining forest extent. To assess how representative our plot network was of the environmental conditions of the wider tropical montane forest biome in Africa, we extracted the environmental data (climate and soil variables used above) at ~1km resolution

from grid-cells that contained montane forest. We then visually compared the distribution of each variable in our dataset to its distribution across the biome.

AfriMont vs global AGC maps

We extracted the AGC estimates for the AfriMont plots (unaggregated, n=666) from four different sources: Harris et al. (ref.[65]) (30 m resolution, 2000 date), the ESA CCI Biomass map[66] (100m resolution, 2017 date), Baccini et al. (ref.[67]) (500m resolution, 2007/8 date) and Avitabile et al. (ref.[68]) (1km resolution, circa 2000-2010 date).
Most of the AfriMont plots were sampled between 2000-2019, see Table S5. Where the plots were found within a single map pixel, we extracted that value. Where plots were larger than the pixel size, we averaged the values from the surrounding pixels weighted according to the proportion of the pixel that was in the plot.

Statistical analysis

Data were analysed using linear mixed-effects models, with site as a random effect. Site was included as a random intercept in all models, and as a random slope where relationships were assessed against elevation. Allowing the slope of the elevation effect to vary amongst sites in this way captures the *a priori* expectation for slopes to differ among sites, for example due to mass elevation effects. The effect of plot size on variation was accounted for by weighting observations by a power transformation of plot size; this was estimated during model fitting using the varPower function in the nlme R package (ref.[69]), and then models refitted using the lme4 R package (ref.[70]) using these estimated weights. Confidence intervals and P-values for mixed effects models parameters were estimated by bootstrapping models (1000 iterations) using the bootstrap_parameters function in the parameters R package (ref.[71]). AGC-stocks, stem density and SD_{70} were natural-log transformed (a small constant was added to SD_{70} before log transforming to avoid log-transforming zeros) to meet assumptions of normality and avoid heteroscedacity. Likewise, the proportional contribution of each size class was square-root transformed. Differences in AGC-stocks between all combinations of lowland and montane forests amongst continents were assessed using Tukey post-hoc tests implemented in the multcomp R package (ref.[72]). Relationships between AGC-stocks and environmental variables were investigated by fitting all subsets of the full model with all environmental covariates and averaging the best supported ($\Delta AIC<4$) models (using dredge and movel.avg functions in the MuMIn R package (ref.[73]). We used these relationships with climate and soil to predict AGC-stocks in each 1km grid-cell containing montane forests (holding topographic variables at their dataset wide mean), and then took the forest-area weighted mean of these to obtain a single mean for the biome. Differences in AGC-stocks between plots with and without elephants were tested using t-test with AGC-stocks natural-log transformed. We investigated if Podocarpaceae abundance (in terms of basal area) and plot AGC-stocks were significantly correlated using Spearman's rank correlation coefficient. To investigate if sampling design affected AfriMont AGC estimates we used ANOVA to test whether site-level mean AGC-stocks differed according to the sampling strategy used to establish plots at that site. To explore the relationship between AfriMont AGC-estimates and global maps, and among these global maps, we used Spearman's correlation test. The same correlation test was used for Lorey's height and AGC.

References Methods

50. Lopez-Gonzalez, G., Lewis, S. L., Burkitt, M. & Phillips, O. L. ForestPlots.net: a web application and research tool to manage and analyse tropical forest plot data. *J. Veg. Sci.* **22**, 610–613 (2011).
51. Lopez-Gonzalez, G., Lewis, S. L., Burkitt, M., Baker, T. R. & Phillips, O. L. ForestPlots.net Database http://www.forestplots.net (2009).
52. Cavanaugh, K., et al. Carbon storage in tropical forests correlates with taxonomic diversity and functional dominance on a global scale. *Global Ecol. Biogeogr.* **23**, 563-573 (2014).
53. Lewis, S. L., et al. 2009 Increasing carbon storage in intact African tropical forests. *Nature* **457**, 1003–1006 (2009).
54. Chave, J. et al. Improved allometric models to estimate the aboveground biomass of tropical trees. *Glob. Change Biol.* **20**, 3177–3190 (2014).
55. Martin, A. R., Doraisami, M. & Thomas, S. C. Global patterns in wood carbon concentration across the world's trees and forests. *Nat. Geosci.* **11**, 915–920 (2018).
56. Chave, J. et al. Towards a worldwide wood economics spectrum. *Ecol. Lett.* **12**, 351–366 (2009).
57. Zanne, A. E. et al. Towards a Worldwide Wood Economics Spectrum https://doi.org/10.5061/dryad.234 (Dryad Digital Repository, 2009).
58. Feldpausch, T. R. et al. Tree height integrated into pantropical forest biomass estimates. *Biogeosciences* **9**, 3381–3403 (2012).
59. Clark, D.A., Brown, S., Kicklighter, D.W., Chambers, J.Q., Thomlinson, J.R., Ni, J. & Holland, E.A. Net primary production in tropical forests: an evaluation and synthesis of existing field data. *Ecol. Appl.* **11**, 371–384 (2001).
60. Paul, T.S.H., Kimberley, M.O. & Beets, P.N. Thinking outside the square: Evidence that plot shape and layout in forest inventories can bias estimates of stand metrics. *Methods Ecol. Evol.* **10**, 381–388 (2019).
61. Fick, S.E. & Hijmans, R.J., WorldClim 2: new 1-km spatial resolution climate surfaces for global land areas. *Int. J. Climatol.* **37**, 4302–4315 (2017).
62. Wilson, A.M. & Jetz, W. Remotely sensed high-resolution Global Cloud Dynamics for predicting ecosystem and biodiversity distributions. *PLoS Biol* **14**(3): e1002415 (2016).
63. Albrecht, R., Goodman, S., Buechler, D., Blakeslee R. & Christian, H. LIS 0.1 Degree Very High Resolution Gridded Lightning Climatology Data Collection. Data sets available online [https://ghrc.nsstc.nasa.gov/pub/lis/climatology/LIS/] from the NASA Global Hydrology Resource Center DAAC, Huntsville, Alabama, U.S.A. doi: http://dx.doi.org/10.5067/LIS/LIS/DATA306
64. Hengl, T., et al. SoilGrids250m: Global gridded soil information based on machine learning. *PLoS ONE* **12**(2): e0169748 (2017).
65. Harris, N. L. et al. Global maps of twenty-first century forest carbon fluxes. *Nat. Clim. Change* **11**, 234–240 (2021).
66. Santoro, M. & Cartus, O. ESA Biomass Climate Change Initiative (Biomass_cci): Global datasets of forest above-ground biomass for the year 2017, v1. Centre for Environmental Data Analysis, 2019. doi:10.5285/bedc59f37c9545c981a839eb552e4084
67. Baccini, A., et al. Estimated carbon dioxide emissions from tropical deforestation improved by carbon-density maps. *Nat. Clim. Change* **2**, 182–185 (2012).
68. Avitabile, V., et al. An integrated pan-tropical biomass map using multiple reference datasets. *Glob. Change Biol.* **22**, 1406–1420 (2016).
69. Pinheiro, J., Bates, D., DebRoy, S., Sarkar, D. & R Core Team. nlme: Linear and Nonlinear Mixed Effects Models. R package version 3.1-151, https://CRAN (2020).
70. Bates, D. Maechler, M., Bolker B. & Walker, S. Fitting Linear Mixed-Effects Models Using lme4. *J. Stat. Softw.* **67**, 1–48 (2015).

71. Lüdecke, D., Ben-Shachar, M., Patil, I. & Makowski, D. Parameters: extracting, computing and exploring the parameters of statistical models using R. *J. Open Source Softw* **5**, 2445 (2020).
72. Hothorn, T., Bretz, F. & Westfall, P. Simultaneous Inference in General Parametric Models. *Biometrical Journal* **50**, 346–363 (2008).
73. Barton, K. 2020. MuMIn: Multi-Model Inference. R package version 1.43.17.
74. Hakizimana, D., Huynen, M.-C. & Hambuckers, A. Structure and floristic composition of Kibira rainforest, Burundi. *Trop. Ecol.* **57**, 739–749 (2016).
75. Sainge, M.N., Lyonga, N.M. & Jailughe, B. Floristic diversify across the Cameroon Mountains: The case of Bakossi National Park and Mt Nlonako. Technical report to the Rufford Small Grant Foundation UK, by Tropical Plant Exploration Group (TroPEG) Cameroon (2018).
76. Hořák, D., et al. Forest structure determines spatial changes in avian communities along an elevational gradient in tropical Africa. *J. Biogeodgr.* **46**, 2466–2478 (2019).
77. Ngute, A.S.K., et al. Investigating above-ground biomass in old-growth and secondary montane forests of the Cameroon Highlands. *Afr. J. Ecol.* **58**, 503–513 (2020).
78. Sainge, M.N., et al. Vegetation, floristic composition and structure of a tropical montane forest in Cameroon. *Bothalia* **49**, 1 (2019).
79. Imani, G., et al. Height-diameter allometry and above ground biomass in tropical montane forests: Insights from the Albertine Rift in Africa. *PLoS ONE* **12**, e0179653 (2017).
80. Schmitt, C.B., Senbeta, S., Woldemariam, T., Rudner, M. & Denich, M. Importance of regional climates for plant species distribution patterns in moist Afromontane forest. *J. Veg. Sci.* **24**, 553–568 (2013).
81. DeVries, B., Avitabile, V., Kooistra, L. & Herold, M. Monitoring the impact of REDD+ implementation in the UNESCO Kafa Biosphere Reserve, Ethiopia. In Proceedings IEEE International Geoscience and Remote Sensing Symposium (IGARSS 2012), 22-27 July, Munich, Germany (pp. 145–146).
82. Hiltner, U., Bräuning, A., Gebrekirstos, A., Huth, A. &Fischer, R. Impacts of precipitation variability on the dynamics of a dry tropical montane forest. *Ecol. Model.* **320**, 92–101 (2016).
83. Maina, E.W., Odera, P.A. & Kinyanjui, M.J. Estimation of Above Ground Biomass in Forests Using Alos Palsar Data in Kericho and Aberdare Ranges. *Open J. forest.* **7**, 79–96 (2017).
84. Cuni-Sanchez, A., et al. New insights on above ground biomass and forest attributes in tropical montane forests. *For. Ecol. Manage.* **399**, 235–246 (2017).
85. Kinyanjui, M.J., Latva-Käyrä, P., Bhuwneshwar, P.S., Kariuki, P., Gichu, A. & Wamichwe, K. An inventory of the above ground biomass in the Mau Forest ecosystem, Kenya. *Open J. Ecol.* **4**, 619–627 (2014).
86. Adhikari, H., Heiskanen, J., Siljander, M., Maeda, E., Heikinheimo, V. & Pellikka, P. K.E. Determinants of aboveground biomass across an Afromontane Landscape Mosaic in Kenya. *Remote Sens*. **9**, 827 (2017).
87. Abiem, I. Arellano, G., Kenfack, D. & Hazel, C., Afromontane forest diversity and the role of grassland-forest transition in tree species distribution. *Diversity* **12**, 30 (2020).
88. Nyirambangutse, B., Zibera, E., Uwizeye, F.K., Nsabimana, D., Bizuru, E., Pleijel, H., Uddling, J., Wallin, G. Carbon stocks and dynamics at different successional stages in an Afromontane tropical forest. Biogeosciences 14, 1285–1303 (2017).
89. Ensslin, A., Rutten, G., Pommer, U., Zimmermann, R., Hemp, A., Fischer, M. Effects of elevation and land use on the biomass of trees, shrubs and herbs at Mount Kilimanjaro. *Ecosphere* **6**, 1–15 (2015).
90. Sheil, D., Jennings, S., Savill, P. Long-term permanent plot observations of vegetation dynamics in Budongo, a Ugandan rain forest. *J. Trop. Ecol.* **16**, 865–882 (2000).
91. Taylor, D., Hamilton, A.C., Lewis, S.L. & Nantale, G. Thirty-eight years of change in a tropical forest: plot data from Mpanga forest reserve, Uganda. *Afr. J. Ecol.* 46, 655–667 (2008).

92. Sheil, D. & Salim, A. Forest tree persistence, elephants, and stem scars. *Biotropica* **36**, 505–521 (2004).

Acknowledgements

We sincerely thank the people of the many villages and local communities who welcomed our field teams and became our field assistants, without whose support the AfriMont dataset would not have been possible. *Cameroon*: villages Elak-Oku, Bokwoango, Bakingili, Muandelengoh, Enyandong, Ekangmbeng, Ngalmoa, Dikome Balue, Muyange, Matamani; assistants: D. Wultof, F. Keming, E. Bafon, J. Meyeih, T. K. Konsum, J. Esembe, F. Luma, F. Teke, E.E. Dagobert, E.D. Ndode, N.F. Njikang; DRC: Bunyakiri, J. Kalume, W. Gului, D. Cirhagaga, B. Mugisho; *Kenya*: assistants: A.M. Aide, H. Lerapo, J. Harugura, R.A. Wamuro, J. Lekatap, L. Lemooli, D. Kimuzi, B.M. Lombo, J. Broas, J. Hietanen, E. Schäfer; *Rwanda*: assistants: I. Rusizana, P. Niyontegereje, J.B. Gakima, F. Ngayabahiga; Tanzania: TEAM staff and affiliates; Uganda: K. Laughlin, X. Mugumya, L. Etwodu, M. Mugisa.

For logistical and administrative support, we are indebted to international, national and local institutions: SOPISDEW, Mt Cameroon National Park, Tropical Plant Exploration Group (TroPEG), Institut Congolais de Conservation de la Nature, Kahuzi-Biega National Park, Itombwe Nature Reserve, NEMA Marsabit Office, Taita Research Station, Kenya Forest Service, Rwanda Development Board, Nyungwe National Park, Conservation International, the Smithsonian Institution, Wildlife Conservation Society, Sokoine University of Agriculture, Tanzania Wildlife Research Institute, Tanzania National Parks Authority, Kilimanjaro National Park, Tanzania Commission for Science and Technology, Royal Zoological Society of Scotland, Uganda Wildlife Authority, Makerere University Biological Field Station, Uganda National Forestry Authority, Uganda National Council for Science and Technology.

Field campaigns for AfriMont were funded by Marie Skłodowska-Curie Actions Intra-European Fellowships (number 328075) and Global Fellowships (number 74356), National Geographic Explorer (NGS-53344R-18), Czech Science Foundation, Rufford Small Grant Foundation (16712-B, 19476-D), Ministry of Foreign Affairs of Finland (BIODEV project), the Academy of Finland (number 318645), Swedish International Development Cooperation Agency, the Strategic Research Area Biodiversity and Ecosystem Services in a Changing Climate, the German Research Foundation (DFG), Gatsby Plants, Natural Science and Engineering Research Council of Canada and International Development Research Centre of Canada.

This paper is also a product of the AfriTRON network, for which we are indebted to hundreds of institutions, field assistants and local communities for establishing and maintaining the plots, including: the Forestry Development Authority of the Government of Liberia, the University of Liberia, University of Ibadan (Nigeria), the University of Abeokuta (Nigeria), the University of Yaounde I (Cameroon), the National Herbarium of Yaounde (Cameroon), the University of Buea (Cameroon), Bioversity International (Cameroon), Salonga National Park (Democratic Republic of Congo), The Centre de Formation et de Recherche en Conservation Forestière (CEFRECOF, Epulu, Democratic Republic of Congo), the Institut National pour l'Étude et la Recherche Agronomiques (INERA, Democratic Republic of Congo), the École Régionale Postuniversitaire d'Aménagement et de Gestion intégrés des Forêts et Territoires tropicaux (ERAIFT Kinshasa, Democratic Republic of

Congo), WWF-Democratic Republic of Congo, WCS-Democratic Republic of Congo, the Université de Kisangani (Democratic Republic of Congo), Université Officielle de Bukavu (Democratic Republic of Congo), Université de Mbujimayi (Democratic Republic of Congo), le Ministère de l'Environnement et Développement Durable (Democratic Republic of Congo), the FORETS project in Yangambi (CIFOR, CGIAR and the European Union; Democratic Republic of Congo), the Lukuru Wildlife Research Foundation (Democratic Republic of Congo), Mbarara University of Science and Technology (MUST, Uganda), WCS-Uganda, the Uganda Forest Department, the Commission of Central African Forests (COMIFAC), the Udzungwa Ecological Monitoring Centre (Tanzania) and the Sokoine University of Agriculture (Tanzania). The AfriTRION network has been supported by the European Research Council (291585, 'T-FORCES' – Tropical Forests in the Changing Earth System, Advanced Grant to O.L.P. and S.L.L.), the Gordon and Betty Moore Foundation, the David and Lucile Packard Foundation, the European Union's Seventh Framework Programme (283080, 'GEOCARBON').

We are particularly grateful to D. Armandu, M. Faustin, T.R. Feldpausch, E. Kearsley, J. Lloyd, R. Lowe, J. Mukinzi, L. Ojo, A.T. Peterson, J. Talbot and L. Zemagho for giving us access to their plot data. We also thank C. Chatelain (Geneva Botanic Gardens) for access to the African Plants Database and to Hao Tang for helping explore the use of GEDI data.

Data from AfriTRON and most of AfriMont are stored and curated by ForestPlots.net, a long-term cyberinfrastructure initiative hosted at the University of Leeds that unites permanent plot records and their contributing scientists from the world's tropical forests. The development of ForestPlots.net and curation of African data have been funded by many sources, including the ERC (principally from AdG 291585 'T-FORCES'), the UK Natural Environment Research Council (including NE/B503384/1, NE/F005806/1, NE/P008755/1, NE/N012542/1 and NE/I028122/1), the Gordon and Betty Moore Foundation ('RAINFOR', 'MonANPeru'), the EU Horizon programme (especially 'GEOCARBON', 'Amazalert') and the Royal Society (University Research Fellowship to S.L.L.).

Author Contributions

A.C-S. conceived the study and assembled the AfriMont dataset. A.C-S. and M.J.P.S. analysed the plot data (with important contributions from S.L.L.). P.P. analysed deforestation trends. S.L.L. conceived and managed the AfriTRON forest plot recensus programme. E.T.A.M. and V.A. helped compare plot data with remote sensing carbon maps. A.C-S. and M.J.P.S. wrote the paper. All co-authors read and approved the manuscript.

Competing interests The authors declare no competing interests.

Data and code availability statement

If this paper is accepted, we will deposit a data package containing plot-level input data and analysis code on ForestPlots.net.

Affiliations

[1]Department of Environment and Geography, University of York, York, UK. [2]Department of International Environmental and Development Studies (NORAGRIC), Norwegian University of Life Sciences, Ås, Norway. [3]Department of Natural Sciences, Manchester Metropolitan University, Manchester, UK. [4]School of Geography, University of Leeds, Leeds, UK. [5]University College London,

Department of Geography, London, UK. [6]Biology Department, Université Officielle de Bukavu, Bukavu, DRC. [7]Service of Wood Biology, Royal Museum for Central Africa, Tervuren, Belgium. [8]Department of Environment, Laboratory of Wood Technology (Woodlab), Ghent University, Ghent, Belgium. [9]University of Jos, Jos, Nigeria. [10]Nigerian Montane Forest Project, Taraba State, Nigeria. [11]Department of Geosciences and Geography, University of Helsinki, Finland. [12]Department of Zoology, Faculty of Science, Charles University, Prague, Czech Republic. [13]Institute of Vertebrate Biology, Czech Academy of Sciences, Brno, Czech Republic. [14]College of Natural and Computational Science, Addis Ababa University, Addis Ababa, Ethiopia. [15]Department of Natural Resource Management, College of Agriculture and Natural Resource, Wolkite University, Wolkite, Ethiopia. [16]European Commission, Joint Research Centre, Ispra, Italy. [17]UK Centre for Ecology & Hydrology, Edinburgh, UK. [18]Université du Cinquantenaire Lwiro, Département de sciences de l'environnement, Kabare, Suk-Kivu, DRC. [19]Isotope Bioscience Laboratory (ISOFYS), Ghent University, Ghent, Belgium. [20]Plant Systematic and Ecology Laboratory, Higher Teachers' Training College, University of Yaoundé I, Yaoundé, Cameroon. [21]Institute of Tropical Forest Conservation, Mbarara University of Science and Technology, Uganda. [22]Biodiversity and Landscape Unit, Gembloux Agro-Bio Tech, Université de Liege, Liège, Belgium. [23]Institut for Geography, Friedrich-Alexander-Universität, Erlangen-Nürnberg, Germany. [24]Institut Supérieur d'Agroforesterie et de Gestion de l'Environnement de Kahuzi-Biega (ISAGE-KB); Département de Eaux et Forêts, Kalehe, DRC. [25]UN Environment World Conservation Monitoring Center (UNEP-WCMC), Cambridge, UK. [26]Computational & Applied Vegetation Ecology (CAVElab), Faculty of Bioscience Engineering, Ghent University, Ghent, Belgium. [27]Department of Anthropology, George Washington University, Washington DC, USA. [28]School of Life Sciences, University of KwaZulu-Natal, Scottsville, Pietermaritzburg, South Africa. [29]Shaanxi Key Laboratory for Animal Conservation, Northwest University, Xi'an, China. [30]International Centre of Biodiversity and Primate Conservation, Dali University, Dali Yunnan, China. [31]University of Canterbury, New Zealand. [32]Inventory & Monitoring Program, National Park Service, Fredericksburg, USA. [33]University of Ghent, Belgium. [34] World Agroforestry (ICRAF), Nairobi, Kenya. [35]Laboratory of Geo-Information Science and Remote Sensing, Wageningen University, Wageningen, the Netherlands. [36]Geography, Environment & Geomatics, University of Guelph, Canada. [37]Institute of Botany of the Czech Academy of Science, Třeboň, Czech Republic. [38]Faculty of Science, University of South Bohemia, České Budějovice, Czech Republic. [39]Université de Montpellier, Montpellier, France.[40]Faculté de Gestion de Ressources Naturelles Renouvelables, Université de Kisangani, Kisangani, DRC. [41]College of Development Studies, Addis Ababa University, Ethiopia. [42]Dendrochronology Laboratory, World Agroforestry Centre (ICRAF), Kenya. [43] Missouri Botanical Garden, St. Louis, Missouri, USA. [44]Department of Biology, University of Burundi, Burundi. [45]Smithsonian Institution Forest Global Earth Observatory (ForestGEO), Smithsonian Tropical Research Institute, Washington DC, USA. [46]Kunming Institute of Botany, Kunming, China. [47]Université Libre de Bruxelles, Brussels, Belgium. [48]Division of Vertebrate Zoology, Yale Peabody Museum of Natural History, New Haven, CT, USA. [49]Institute for Atmospheric and Earth System Research, Faculty of Science, University of Helsinki, Finland. [50]Department of Plant Systematics, University of Bayreuth, Germany.[51]Institute for Geography, Friedrich-Alexander-University Erlangen-Nuremberg, Germany. [52]Helmholtz-Centre for Environmental Research (UFZ), Leipzig, Germany. [53]Department of Ecology, Faculty of Science, Charles University, Prague, Czech Republic. [54]International Gorilla Conservation Programme, Musanze, Rwanda. [55]Department of Natural Resources, Karatina University, Kenya. [56]Dept. Ecosystem Science & Sustainability, Colorado State University, Fort Collins, USA. [57]Eco2librium LLC, Boise, USA. [58]Department of Ecology, Université de Kisangani, Kisangani, DRC. [59]Environmental Change Institute, School of Geography and the Environment, University of Oxford, Oxford, UK. [60]Tropical Forests and People Research Centre, University of the Sunshine Coast, Australia. [61]Flamingo Land Ltd., North Yorkshire, UK. [62]College of African Wildlife Management, Mweka, Tanzania. [63]School of GeoSciences, University of Edinburgh, UK. [64]Department of Geography and Environmental Sciences, University of Dundee, Dundee, UK. [65]Independent Botanist, Harare, Zimbabwe. [66]Department of Horticultural Sciences, Faculty of Applied Sciences, Cape Peninsula University of Technology, Bellville, South Africa. [67]Biology

Department, University of Rwanda, Rwanda . [68]Department of Biological and Environmental Sciences, University of Gothenburg, Sweden. [69]Mountains of the Moon University, Fort Portal, Uganda. [70]National Agricultural Research Organisation, Mbarara Zonal Agricultural Research and Development Institute, Mbarara, Uganda. [71]School of Biological Sciences, University of Southampton, Southampton, UK. [72]Conservation Science Group, Department of Zoology, University of Cambridge, Cambridge, UK. [73]State Key Laboratory of Information Engineering in Surveying, Mapping and Remote Sensing, Wuhan University, China. [74]Key Biodiversity Areas Secretariat, BirdLife International, Cambridge, UK. [75]School of Life Sciences, University of Lincoln, UK. [76]Department of Biology, University of Florence, Sesto Fiorentino, Italy. [77]Tropical Biodiversity Section, Museo delle Scienze, Trento, Italy. [78]Tropical Plant Exploration Group (TroPEG) Cameroon. [79]Center for Development Research (ZEF), University of Bonn, Germany. [80]Conservation and Landscape Ecology, University of Freiburg, Germany.[81]Applied Biology and Ecology Research Unit, University of Dschang, Dschang, Cameroon. [82]Department of Ecology and Natural Resource Management, Norwegian University of Life Sciences, Norway. [83]Water and Land Resources Center, Addis Ababa University, Addis Ababa, Ethiopia. [84]African Wildlife Foundation (AWF), Biodiversity Conservation and Landscape Management Program, Simien Mountains National Park, Debark, Ethiopia. [85]Faculty of Forestry, University of British Columbia, Vancouver, Canada. [86]Center for International Forestry Research (CIFOR), Bogor, Indonesia. [87]Department of Forest Ecology, Faculty of Forestry and Wood Sciences, Czech University of Life Sciences, Prague, Czech Republic. [88]Department of Plant Biology, Faculty of Sciences, University of Yaoundé I, Cameroon. [89]Bioversity International, Yaoundé, Cameroon. [90]UK Research & Innovation, UK. [91]Department of Geography, National University of Singapore, Singapore. [92]Faculty of Forestry, University of Toronto, Toronto, Canada.[93]Biodiversity Foundation for Africa, East Dean, East Sussex, UK. [94]Forestry Development Authority of the Government of Liberia (FDA), Monrovia, Liberia. [95]School of Forestry and Environmental Studies, Yale University, New Haven, USA. [96]Department of Biological Sciences, Florida International University, Florida, USA. [97]School of Natural Sciences, University of Bangor, Bangor, UK. [98]University of Liberia, Monrovia, Liberia. *corresponding author: a.cuni-sanchez@york.ac.uk

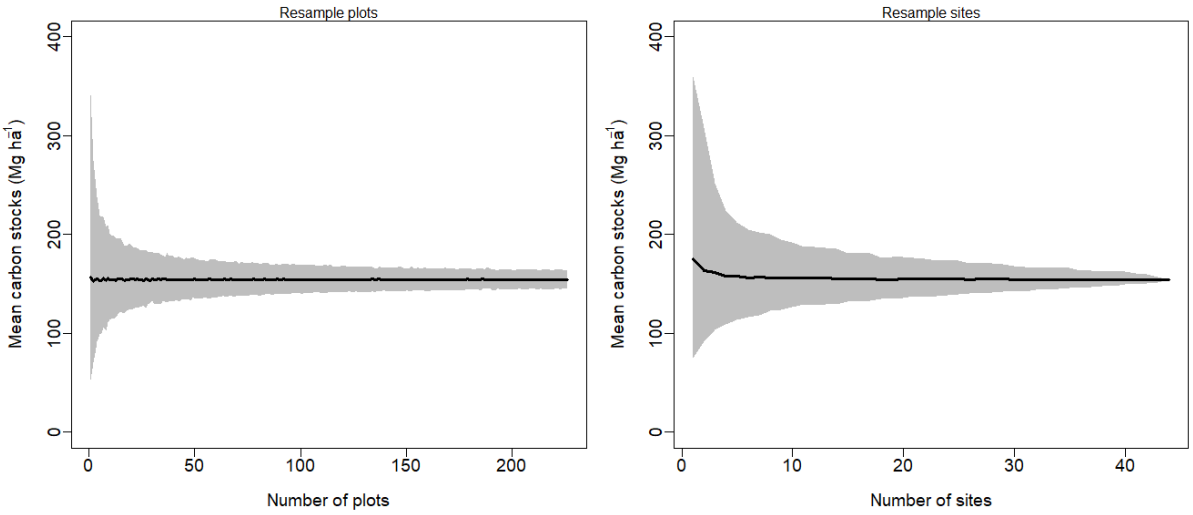

Fig. S1. Sensitivity of our mean aboveground carbon stock estimates to data subsampling. Data were resampled at different sample sizes either at plot level (sampling with replacement) or at site level (sampling without replacement). N = 1000 resamples for each sample size.

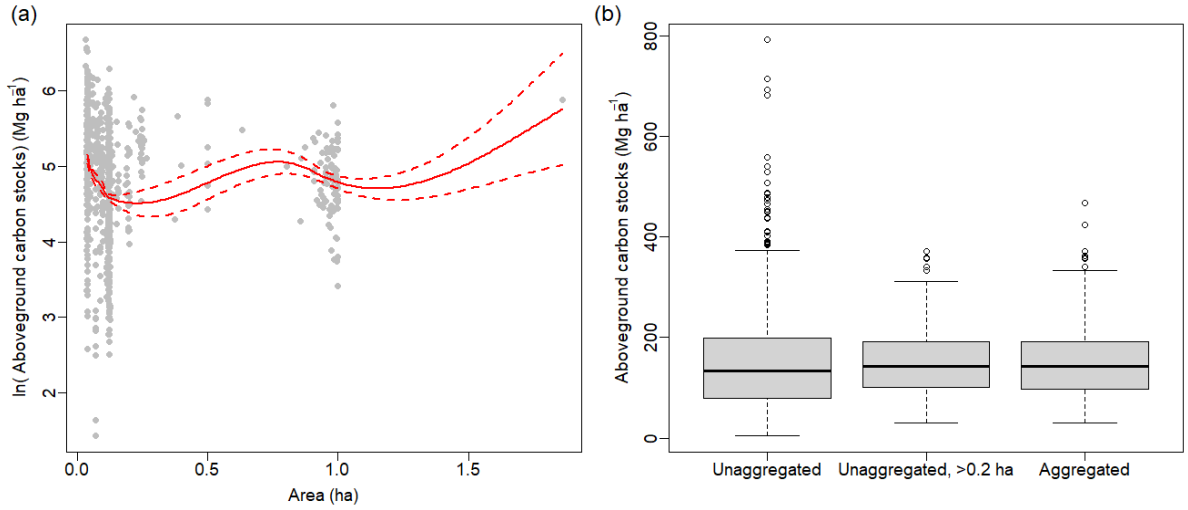

Fig. S2. Effect of plot area and aggregation procedure for nearby small plots on estimates of aboveground carbon stocks. (a) Relationship between aboveground carbon stocks and plot area of plots prior to aggregation. The red line shows the fit of a locally weighted regression model (span = 0.75) relating these variables, with dashed lines showing the standard errors. (b) Variation in aboveground carbon stocks of montane forests in Africa using either all plots prior to aggregation (unaggregated), plots prior to aggregation but excluding those < 0.2 ha (unaggregated, >0.2 ha) or the aggregated plots used in the main analyses (aggregated).

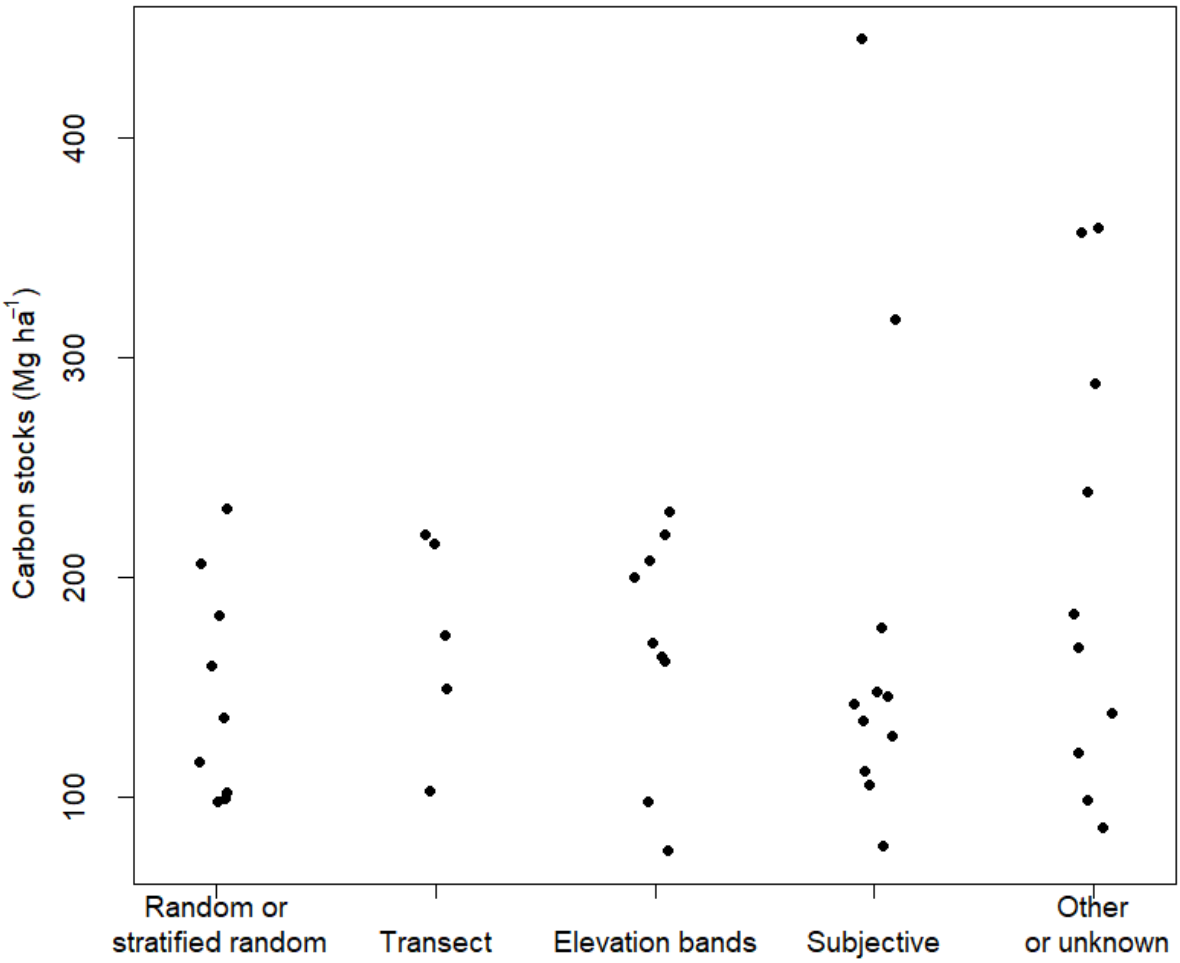

Fig. S3. Effects of plot design on aboveground carbon (AGC) stocks (each site represents one dot). Sampling strategies include random or stratified random, plots positioned along transects, plots established within elevation bands, subjective measures such as choosing an area of forest considered representative of the wider area, and other strategies (1 plot sampled per site or unclear strategy). Carbon stocks (log-transformed) did not differ significantly between sites with different sampling strategies (ANOVA: $F_{4,39} = 0.432$, $P = 0.785$). For specific site information see Table S5.

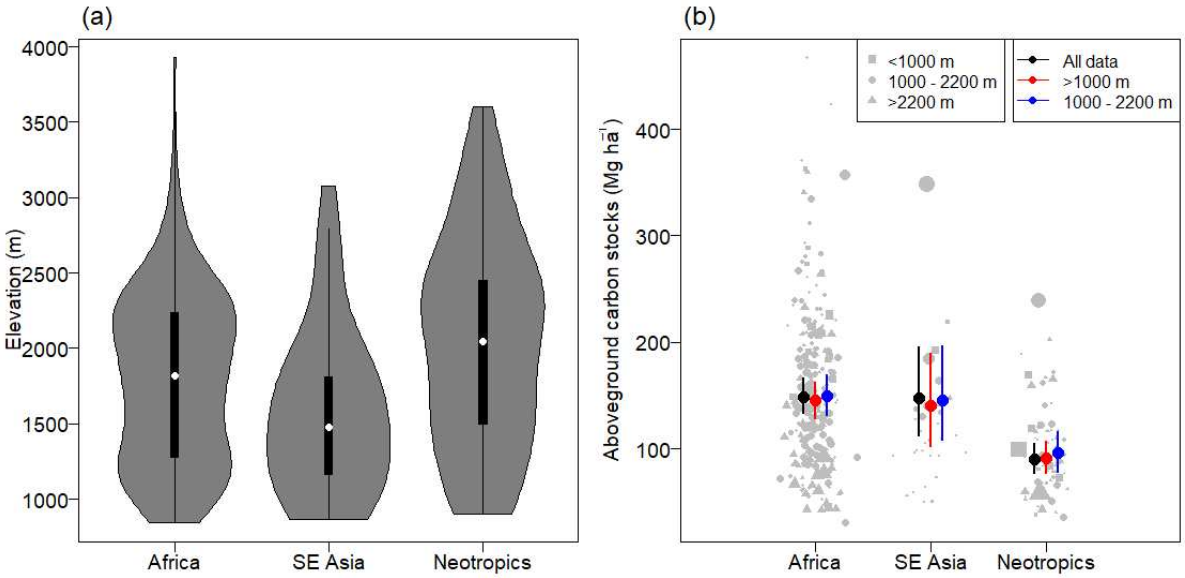

Fig. S4. Robustness of differences in tropical montane forest aboveground carbon (AGC) stocks among continents to differences in elevation. (a) Elevations of montane forests sampled in each continent. Violin plots show the distribution of data, with boxplots showing the median and interquartile range of elevation in each continent. (b) Effect of removing submontane plots (800-1000 m asl) and high elevation plots (> 2200 m asl, approximately the upper quartile of elevations for the African montane plot dataset) on AGC-stocks in montane forests in each continent. Mean AGC-stocks and 95% confidence intervals are shown as estimated by models using i) all data, ii) excluding plots 800-1000 m, and iii) restricting plots to 1000-2200 m. Means for all plots differ from the analysis in Fig. 1 as literature plots without elevation data (plots in Colombia) were excluded from this analysis. Point symbols are proportional to square-root plot area. N = 324 plots.

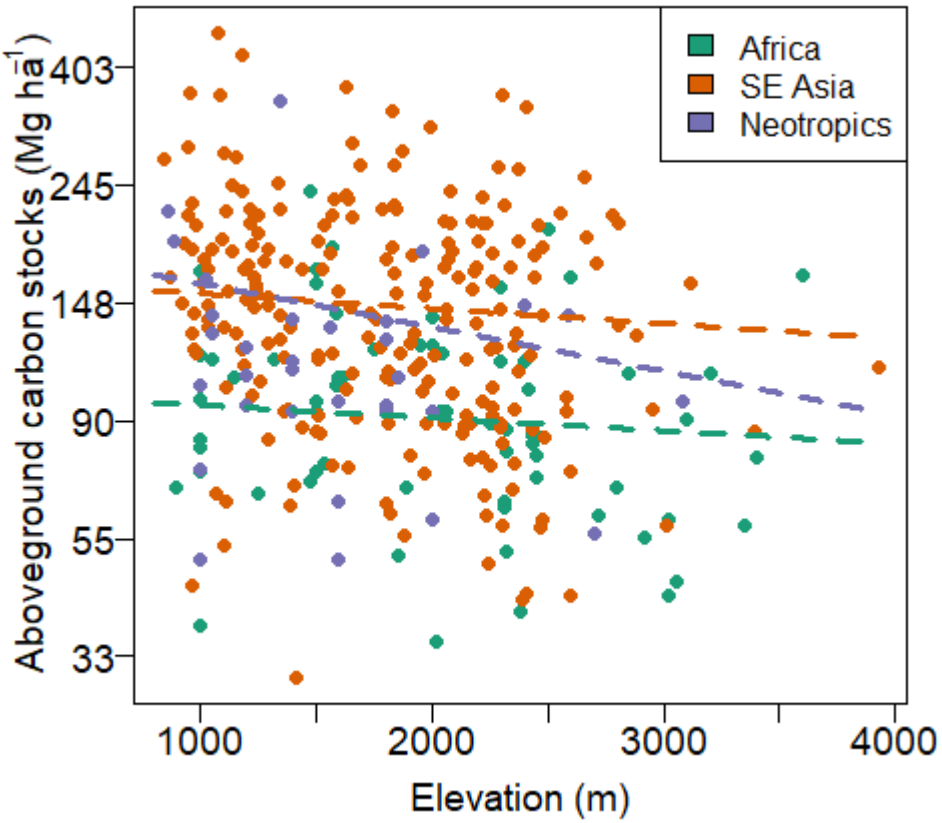

Fig. S5. Relationship between aboveground carbon (AGC) stocks and elevation for tropical montane forests in each continent. Dashed lines show relationships from a linear mixed-effects model of log-transformed AGC-stocks as a function of elevation, continent and their interaction. Site was included as a random effect, and AGC-stock – elevation relationships allowed to vary among sites. Lines show fitted slopes across sites. Neither the overall relationship between elevation and AGC-stocks (slope = -0.039 [95% CI = -0.127 – 0.057], *P* = 0.420) nor interactions between elevation and continent (Southeast Asia, change in slope = -0.074 [-0.294 – 0.149], *P* = 0.503; Neotropics, change in slope = 0.006 [-0.132 – 0.149], *P* = 0.913) are statistically significant. N = 324 plots.

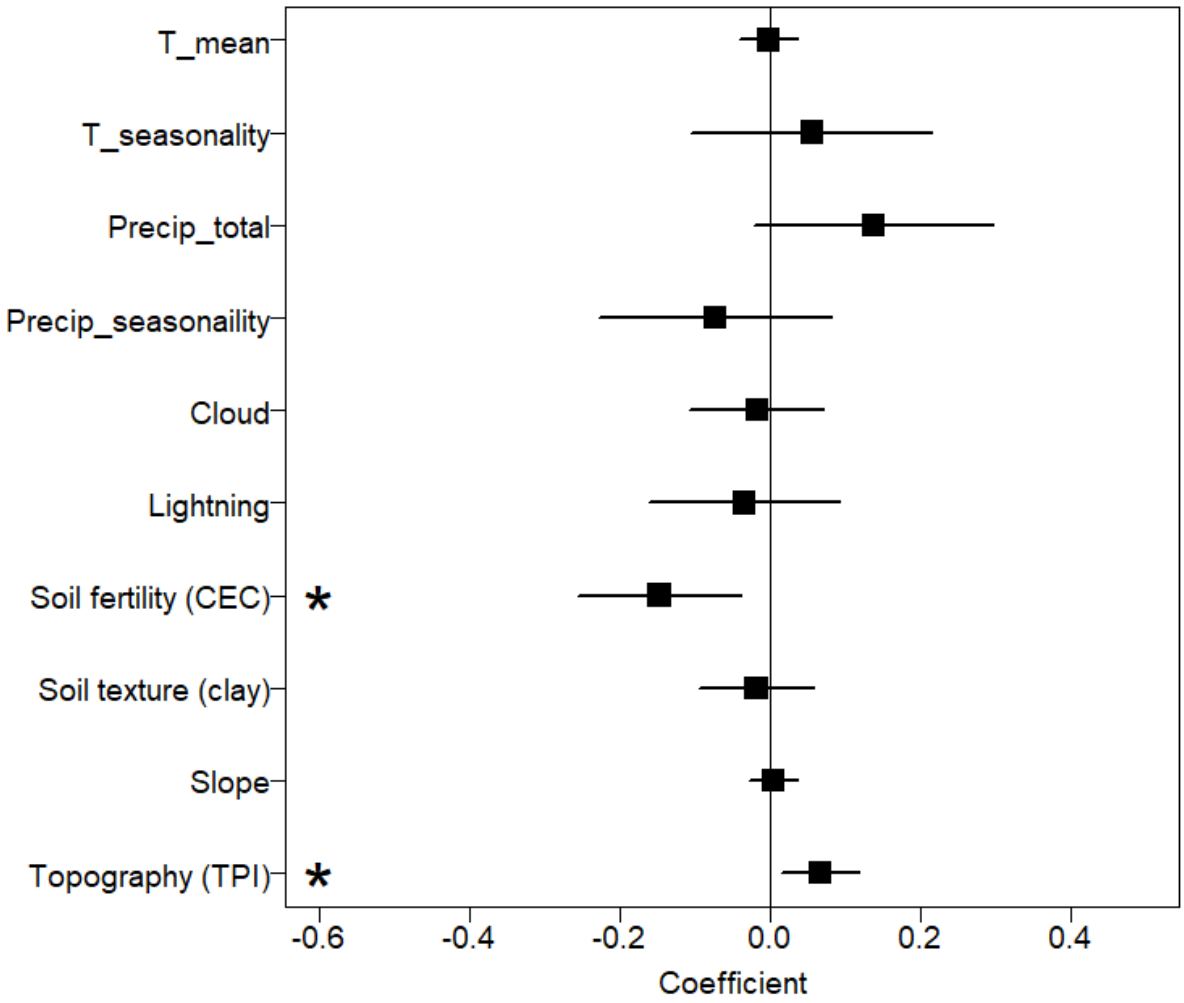

Fig. S6. Environmental drivers of aboveground carbon stocks across sites. Coefficients are from a linear mixed effect model with site as a random intercept. Results are following all-subsets regression and model averaging, in which variables that do not appear in well supported models are given coefficients of zero, leading to shrinkage in model coefficients. Statistically significant relationships ($P < 0.05$) are indicated with asterisks. TPI refers to topographic position index (positive values indicate higher than surroundings, negative values indicate lower than surroundings).

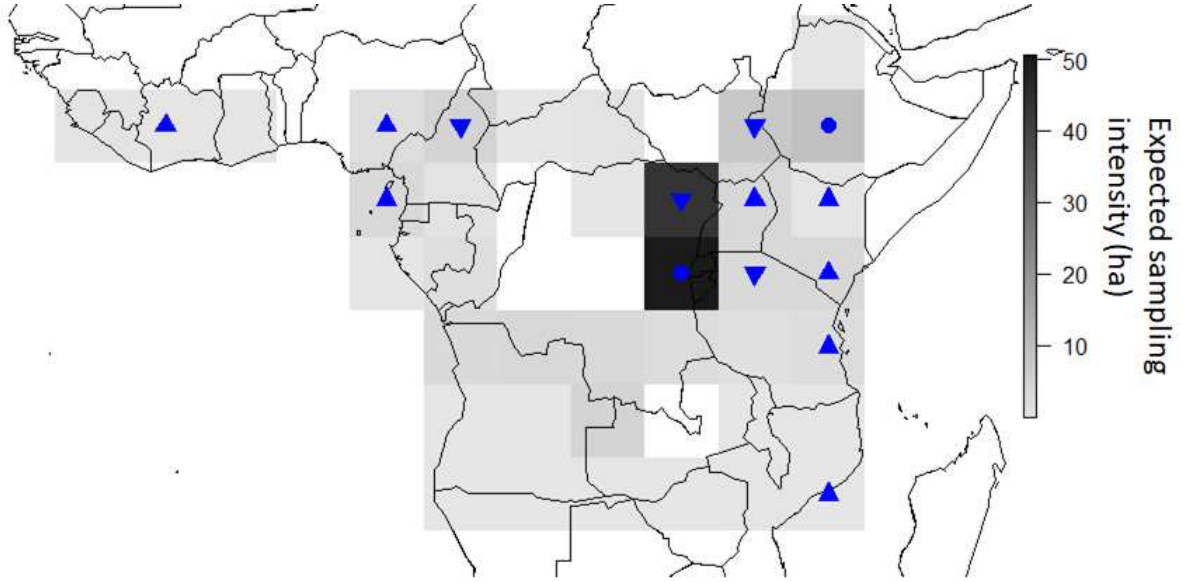

Fig. S7. Expected sampling effort (in ha) if effort was distributed in proportion to the area of montane forest biome. Data are summarised at 10 degree resolution. Upward triangles show grid-cells where AfriMont sampling effort is more than double expected effort, downward triangles are where AfriMont sampling effort is less than half expected effort. Circles denote AfriMont sampling effort being between half and double expected effort. The extent of the tropical montane forest biome was defined as forests > 800m asl, forest cover in December 2018 extracted from ref.[36], clipped to 'primary humid forest' using ref.[37].

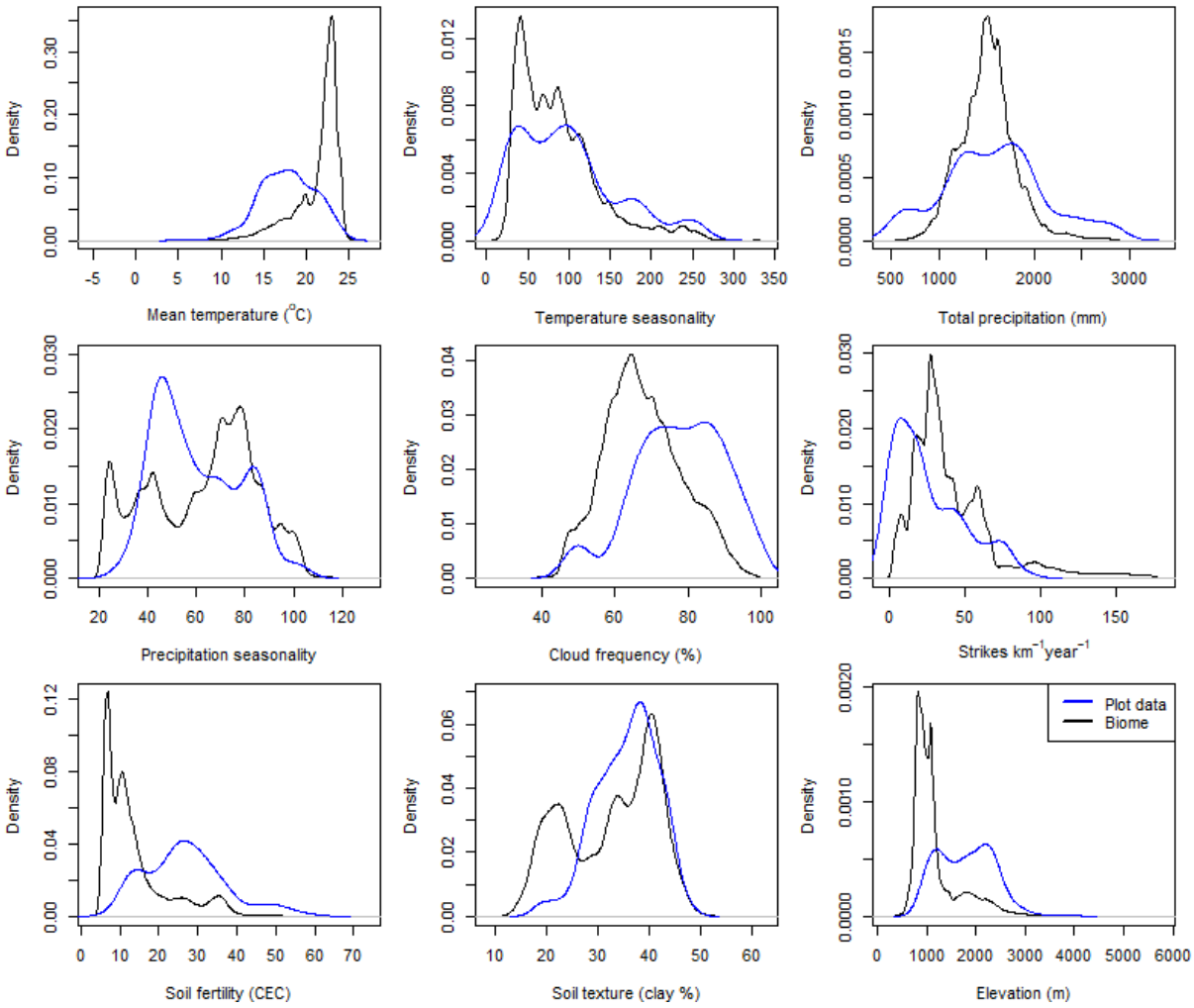

Fig. S8. Differences in the environmental conditions sampled by AfriMont plot data and the tropical montane forest biome in Africa. The extent of the biome was defined as forests > 800m asl, forest cover in December 2018 extracted from ref.[36], clipped to 'primary humid forest' using ref.[37]. Environmental variables for the biome were extracted at ~1km resolution.

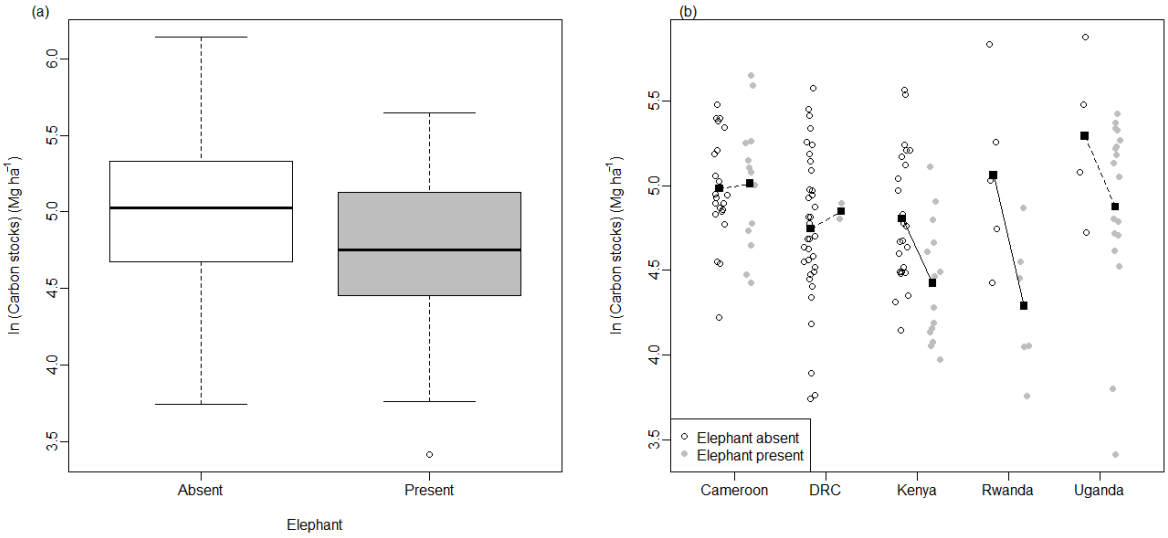

Fig. S9. Differences in aboveground carbon stocks in plots located in montane forests with and without elephants. (a) Differences across all plots in the AfriMont dataset. Carbon stocks are statistically significantly lower in forests with elephants (t-test, t = 3.5, df=83.5, p = 0.001). (b) Differences in countries where elephants are present in at least one of the montane site studied. Black squares show means in each country in forests with or without elephants – solid lines denote statistically significant differences (t-tests, $p < 0.05$). Elephant presence in 2019 was estimated by co-authors (see Table S5).

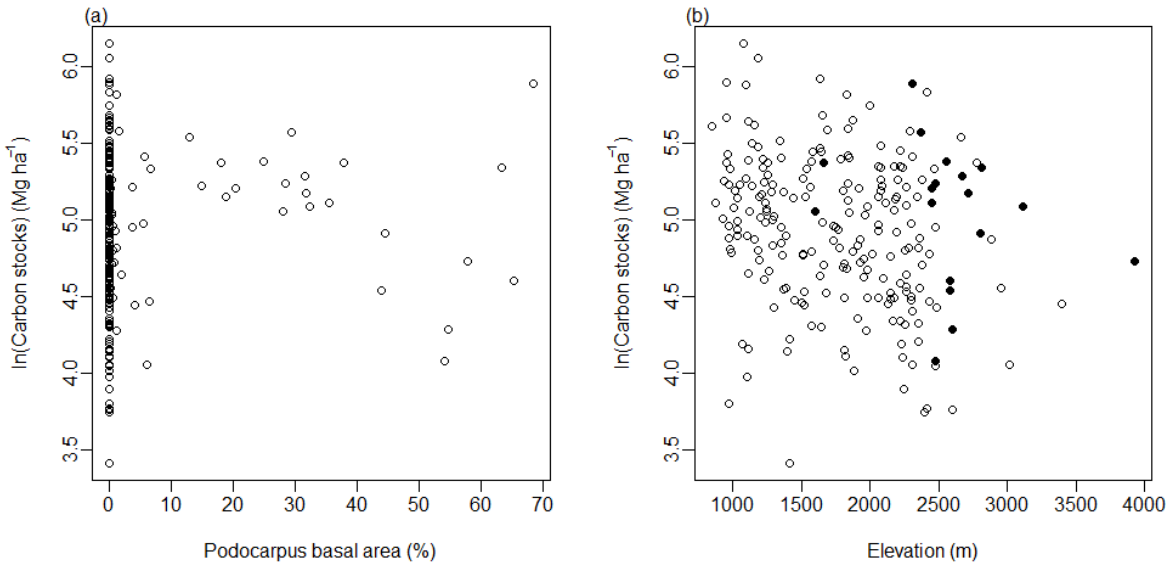

Fig. S10. (a) Relationship between aboveground carbon (AGC) stocks and Podocarpaceae basal area, expressed as a percentage of total plot basal area. These variables are not significantly correlated (rs = 0.083, n = 226, p = 0.212). (b) Distribution of plots with at least 20% basal area of Podocarpaceae (black points) in relation to elevation and AGC-stocks. AGC-stocks are not significantly related to elevation or Podocarpaceae basal area (Linear mixed effects model, p = 0.152 and 0.132 respectively).

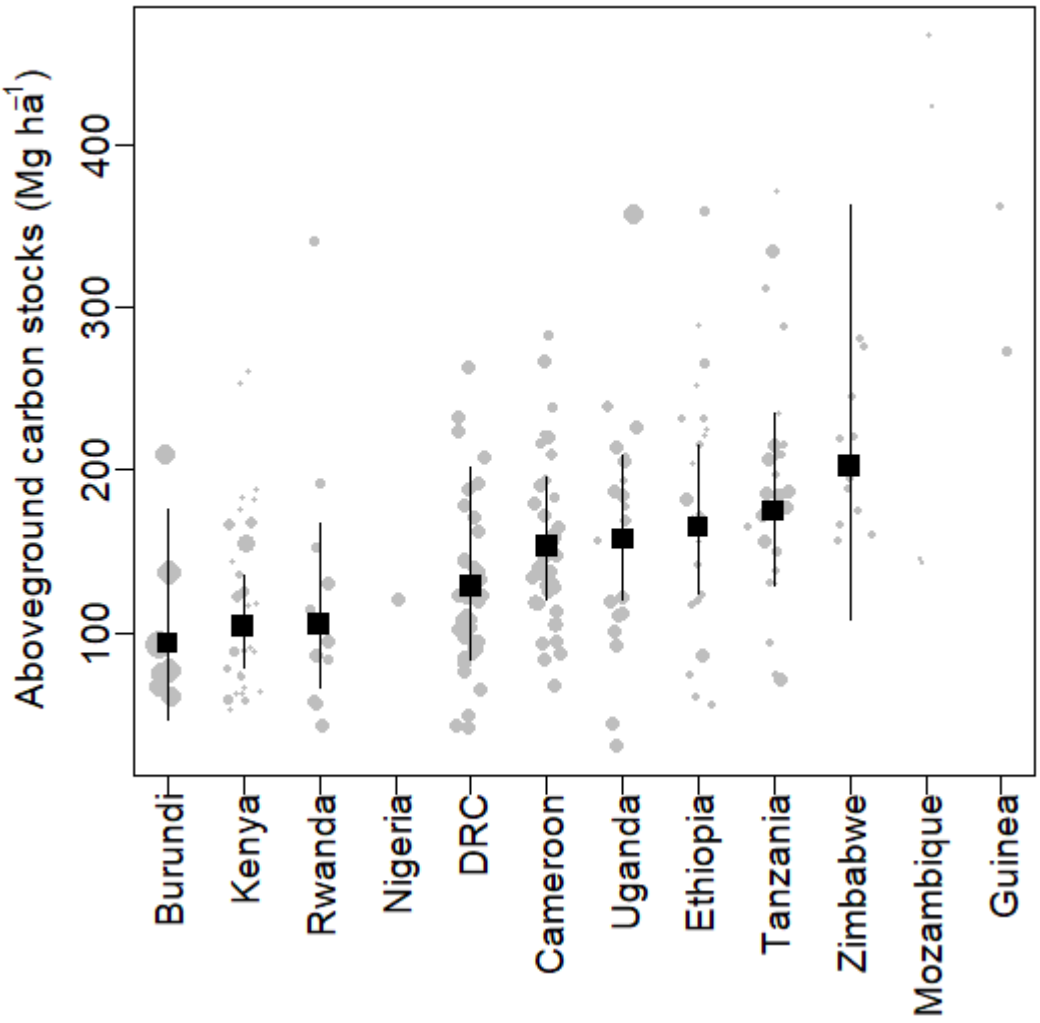

962
963 **Fig. S11.** Within country variation in aboveground carbon stocks. Error bars show means and
964 95% confidence intervals estimated by mixed effects models. Modelled means have not
965 been shown for countries with fewer than five plots. Point size is proportional to plot area.
966
967

Table S1 Correlations between different recent remote sensing derived carbon maps and between these maps and AfriMont plot aboveground carbon (AGC) stock estimates.

		Date	Spatial resolution	1	2	3	4
1	Harris et al. (ref. [65])	2000	30m	-			
2	ESA CCI Biomass map (ref. [66])	2017	100m	**0.29**			
3	Baccini et al. (ref. [67])	2007/2008	500m	0.04	**0.35**		
4	Avitabile et al. (ref. [68])	2000-2010	1km	**0.09**	**0.45**	**0.59**	
5	AfriMont plots (unaggregated, n=666)			**0.19**	-0.11	**-0.13**	**-0.12**

bold: significant at P<0.01

Table S2 Estimated differences in aboveground carbon (AGC) stocks amongst continents and forest elevation category. Coefficients are from a linear mixed effect model, where African montane forests are taken as the model intercept; other coefficients show differences from this intercept. 95% confidence intervals and P-values were estimated by bootstrapping the fitted model. AGC-stocks were log-transformed prior to analysis, and coefficients relate to the log-transformed variable.

Term	Estimate	LCL	UCL	P
Intercept - Africa montane	5.007	4.921	5.101	<0.001
Difference:				
Africa lowland	0.054	-0.066	0.170	0.360
Southeast Asia montane	-0.037	-0.287	0.202	0.793
Southeast Asia lowland	0.311	0.142	0.472	<0.001
Neotropics montane	-0.531	-0.655	-0.411	<0.001
Neotropics lowland	-0.276	-0.386	-0.175	<0.001

Table S3. Difference in contribution of different size classes to aboveground carbon (AGC) stocks and number of stems between montane and lowland forests in Africa. Coefficients are from linear mixed effects models of the proportion contribution of a given size class against forest elevation category are shown. Proportions were square-root transformed prior to analysis, and coefficients relate to the transformed variables. 95% confidence intervals and P-values were estimated by bootstrapping the fitted models.

Variable	Size class	Difference from lowland	LCL	UCL	P
AGC-stocks	<30	-0.018	-0.071	0.031	0.474
	30-50	-0.004	-0.044	0.036	0.835
	50-70	-0.024	-0.066	0.016	0.240
	>70	-0.011	-0.100	0.075	0.799
Stems	<30	-0.031	-0.059	-0.004	0.026
	30-50	0.030	0.003	0.056	0.022
	50-70	0.014	-0.015	0.044	0.378
	>70	0.018	-0.019	0.055	0.334

Table S4. Relationship between elevation and aboveground carbon (AGC) stocks, stem density and density of large stems (>70 cm diameter, SD_{70}) for the AfriMont dataset. Relationships are from linear mixed-effects models with site as a random effect, and relationship with elevation allowed to vary with site. Response variables were log-transformed, and elevation was scaled by subtracting its mean and dividing by its standard deviation. 95% confidence intervals and P values were obtained by bootstrapping the fitted models. Polynomial and linear models were compared using likelihood ratio tests; slopes are from linear models. RWE: Rwenzori Mts, VIR: Virunga Mts, see Table S5.

	All data					**Excluding RWE and VIR**				
Response variable	**Slope**	**LCL**	**UCL**	**P**	**Significance of non-linear relationship**	**Slope**	**LCL**	**UCL**	**P**	**Significance of non-linear relationship**
AGC-stocks	-0.043	-0.140	0.064	0.418	χ^2_1 = 0.129, P =0.720	-0.039	-0.154	0.076	0.511	χ^2_1 = 0.440, P = 0.507
Stem density	-0.036	-0.118	0.042	0.350	χ^2_1 0.002, P = 0.963	-0.044	-0.135	0.046	0.308	χ^2_1 = 0.142, P = 0.706
SD_{70}	-0.059	-0.260	0.148	0.599	χ^2_1 = 0.105, P = 0.746	0.022	-0.202	0.236	0.849	χ^2_1 = 4.005, P = 0.045*

* Polynomial model: $SD_{70} = 2.756 – 0.575\ Elevation + 2.060\ Elevation^2$

Table S5 Site attributes of the AfriMont dataset. Plots size refers to planimetric area. Elevation from SRTM v3 at 1 arc-sec (~30m) resolution.

Country	Site	Code	No. plots	Plots size (ha)		Elevation (m asl)	Elephant Presence	Year	Plot Setup	Main reference
Burundi	Kibira NP	BUR	7	1.8-3.6	a	1900-2500	0	2012	T	Ref. [74]
Cameroon	Babanki	BAB	2	0.72-1	a	2000-2350	0	2008-2009	R	unpublished
	Bakossi Mts	BAK	12	0.91-0.99		1000-1400	0	2016	Sub	Ref. [75]
	Mt Cameroon	CAM	10	0.5-1.1	a	960-2270	1 (some)	2011	T	Ref. [76]
	Mt Mbam	MBA	2	0.23-0.54	a	1760-2220	0	2017	E	Ref. [77]
	Nguti	NGI	3	0.80-0.87		870-940	1	2013	other	unpublished
	Mt Oku	OKU	2	0.39-0.54	a	2200-2700	0	2017	E	Ref. [77]
	Rumpi Hills	RUM	4	0.95-0.99		1350-1750	0	2015	Sub	Ref. [78]
	Takamanda	TNP	2	1		1190-1290	1	2012	other	Ref. [5]
DRC	Itombwe Mts	ITO	8	0.9		1100-2470	1 (some)	2019	E	unpublished
	Kahuzi-Biega NP	KAH	29	0.9		1630-2430	0	2014	R	Ref. [79]
Ethiopia	Bonga	BON	5	0.19-0.82	a	1570-2660	0	2001-2005	T	Ref. [80]
	Harena Forest (Bale)	HAR	4	0.19-0.27	a	800-1120	0	2001-2005	T	Ref. [80]
	Jaba	JAB	1	0.26	a	1500-1650	0	2001-2005	R	Ref. [80]
	Kafa Biosphere Reserve	KAF	7	0.24-0.35	a	1470-2670	0	2011	R	Ref. [81]
	Munessa Forest (Bale)	KUK	1	0.49	a	2300-2310	0	2011	other	Ref. [82]

	Berhane–Kontir	SHE	6	0.19-0.23	a	1520-2090	0	2001-2005	T	Ref. [80]
	Yayu Coffee Forest	YAY	1	0.99		1500	0	2014	other	unpublished
Guinea	Mt Nimba	NIM	2	0.36-0.42	a	760-1060	0	2011	Sub	unpublished
Kenya	Aberdares Mts	ABE	5	0.35-0.77	a	2270-3020	1	2014	R	Ref. [83]
	Mt Kulal	KUL	9	0.2		1800-2150	0	2016	E	Ref. [84]
	Mt Marsabit	MAR	6	0.2		1070-1400	1	2016	E	Ref. [84]
	Mau Forest Complex	MAU	3	0.27-0.45	a	2080-2850	1	2012	R	Ref. [85]
	Mt Nyiro	NYI	9	0.2		2150-2710	0	2016	E	Ref. [84]
	Taita Hills	TAI	6	0.2-1.6	a	1550-2170	0	2013-2015	R	Ref. [86]
Mozambique	Mt Lico	LIC	1	0.11	a	900-1000	0	2018	Sub	unpublished
	Mt Mabu	MAB	2	0.11-0.18	a	1000-1320	0	2008	Sub	unpublished
	Mt Muli	MUL	1	0.11	a	1200-1280	0	2018	Sub	unpublished
Nigeria	Ngel-Nyaki FR	NGE	1	1		1570	0	2015	other	Ref. [87]
Rwanda	Nyungwe NP	NYU	5	0.5		1950-2480	0	2015	Sub	Ref. [88]
	Virunga Mts	VIR	6	0.99		2470-3390	1	2015	Sub	unpublished (TEAM)
Tanzania	Nguu	GUU	1	0.38		950	0	2009	other	Ref. [12]
	Mt Kilimanjaro	KIL	13	0.19-0.25		1630-2800	0	2010-2013	E	Ref. [89]
	Udzungwa Mts	UDZ	7	0.85-0.97		1140-1970	0	2007-2010	E	Ref. [12]
	Ukaguru	UKA	2	0.37-0.39		1190-1640	0	2009	Sub	Ref. [12]

	Uluguru	ULU	2	0.18-0.26		970-2110	0	2009	Sub	Ref. [12]
	Usambara Mts	USA	4	0.97-0.99		1050-1830	0	2010	E	Ref. [12]
Uganda	Budongo FR	BUD	1	1.86		1090	0	2008	other	Ref. [90]
	Bwindi NP	BWI	6	1		1420-2380	1	2009	Sub	Ref. [52]
	Kibale NP	KIB	4	0.24		1210-1540	1	2013	other	Ref. [46]
	Mpanga	MPG	1	0.63		1180	0	2006	other	Ref. [91]
	Rabongo FR	RAB	7	1		950-990	1	1992-1993	R	Ref. [92]
	Rwenzori Mts	RWE	4	0.61-0.86	a	1800-3900	1 (some)	2019	E	unpublished
Zimbabwe	Chirinda FR	CHI	12	0.24		1090-1250	0	1995	R	unpublished

[a] plots were originally <0.2 ha and were aggregated into larger plots, see methods for details. Elevation for these plots refers to original unaggregated plots.

FR: Forest Reserve, NP: National Park.

For elephant presence: 1: presence in all plots in the site, some: some plots in the site, 0: absence. Presence in 2019 was estimated by co-authors and refers to variable densities of resident and migrant individuals of both the savanna elephant (*Loxodonta africana*) and the smaller forest elephant (*L. cyclotis*). In some sites elephants are confined and highly abundant (e.g. in ABE, where there is an electric fence), conditions which might not have occurred under 'natural' circumstances in the past.

Plot setup refers to: random or stratified random (R), plots positioned along transects (T), plots established within elevation bands (E), subjective measures such as choosing an area of forest considered representative of the wider area (Sub), and other strategies (1 plot sampled per site or unclear strategy, other).

Table S6 Information on the AfriTRON plots used.

Country	Code	Latitude	Longitude	Elevation (m asl)	Plot size (ha)
Cameroon	DJL-01	3.1	13.6	544	1
	DJL-02	3.1	13.6	606	1
	DJL-03	3	13.6	569	1
	DJL-04	3	13.6	595	1
	DJL-05	3	13.6	604	1
	DJL-06	3	13.6	585	1
	DJA-05	3.2	12.6	640	1
	DJA-07	2.9	13.3	580	0.5
	DJA-09	3.1	13.6	660	1
	CAM-02	2.3	9.9	38	1
	EJA-04	5.7	9	142	1
	EJA-05	5.7	9	166	1
	NGI-12	5.2	9.7	724	1
	NGO-04	2.6	14.1	491	1
	NGO-01	2.6	14.1	516	1
	NGO-02	2.6	14.1	574	1
	NGO-05	2.6	14.1	518	1
	NGO-06	2.6	14.1	529	1
	DNG-02	5.2	13.5	716	1
	MIT-01	2.4	13.5	618	1
	DJA-01	3.3	12.9	590	2.25
	DJA-02	3.3	12.9	590	2.5
	DJA-03	3.3	12.9	570	2.5
	DJA-04	3.3	12.9	610	2.5
	CAM-01	2.3	9.9	58	1
	CAM-03	2.4	9.9	100	1

DJK-01	3.3	12.7	647	1
DJK-02	3.3	12.7	722	1
DJK-03	3.4	12.7	639	1
DJK-04	3.4	12.7	639	1
DJK-05	3.3	12.8	779	1
DJA-17	2.9	13.3	575	0.2
TNP-11	6.2	9.3	166	0.92
DJK-06	3.3	12.8	639	1
TNP-14	6.1	9.3	158	0.8
MDJ-01	6.2	12.8	789	1
MDJ-03	6	12.9	757	1
MDJ-07	6	12.9	764	1
MDJ-10	6	12.9	767	0.4
BIS-01	3.3	12.5	633	1
BIS-02	3.3	12.5	633	1
BIS-03	3.3	12.5	660	1
BIS-04	3.3	12.5	634	1
BIS-05	3.3	12.5	658	1
BIS-06	3.3	12.5	574	1
TNP-06	6.1	9.4	187	1
TNP-07	6.1	9.4	381	1
TNP-10	6.2	9.3	185	1
TNP-12	6.1	9.2	133	1
TNP-13	6.1	9.2	139	1
TNP-15	6.1	9.3	182	1
NGI-01	5.3	9.5	248	1
NGI-02	5.3	9.5	258	1
NGI-03	5.4	9.6	251	1
NGI-04	5.4	9.6	511	1
NGI-05	5.4	9.6	397	1

	NGI-06	5.2	9.7	531	1
	NGI-07	5.2	9.7	790	1
	NGI-08	5.2	9.7	669	1
DRC	YOK	0.3	25.3	418	9
	ITU-01	1.4	28.4	750	0.25
	ITU-02	1.4	28.5	750	0.44
	ITU-03	1.3	28.6	750	0.5
	ITU-04	1.4	28.4	750	0.5
	ITU-05	1.4	28.5	750	0.5
	ITU-06	1.4	28.6	750	0.5
	SNG-01	-1.7	20.6	371	1
	SNG-02	-1.7	20.6	365	1
	SNG-03	-1.7	20.6	420	1
	SNG-04	-1.7	20.5	384	1
	SNG-05	-1.7	20.5	361	1
	SNG-06	-1.7	20.5	360	1
	SNG-07	-1.7	20.5	362	1
	SNG-08	-1.7	20.5	382	1
	SNG-09	-1.7	20.5	374	1
	KSN-01	0.3	25.3	449	0.2
	KSN-02	0.3	25.3	455	0.2
	KSN-05	0.3	25.3	452	0.2
	KSN-06	0.3	25.3	440	0.2
	YGB-08	0.8	24.5	460	1.02
	YGB-14	0.8	24.5	438	1.07
	YGB-15	0.8	24.5	464	1.07
	YGB-16	0.8	24.5	427	1.02
	YGB-17	0.8	24.5	466	1.03
	YGB-18	0.9	24.5	427	1.01
	YGB-24	0.8	24.5	464	1.07

	YGB-25	0.8	24.5	477	0.99
	YGB-26	0.8	24.5	435	1
	YGB-27	0.8	24.5	417	1
	YGB-28	0.8	24.5	489	1.02
Liberia	GBO-19	5.4	-7.6	175	0.78
	GBO-02	5.4	-7.6	172	1
	GBO-08	5.4	-7.6	174	1
	GBO-01	5.4	-7.6	171	0.98
	GBO-03	5.4	-7.6	175	0.69
	GBO-04	5.4	-7.6	175	0.42
	GBO-10	5.4	-7.6	175	0.46
	GBO-11	5.4	-7.6	175	0.67
	GBO-13	5.4	-7.6	175	0.56
	GBO-14	5.4	-7.6	175	0.83
	GBO-15	5.4	-7.6	175	0.71
	GBO-16	5.4	-7.6	161	0.44
	GBO-18	5.4	-7.6	175	0.62
	GBO-20	5.4	-7.6	175	0.59
	CVL-01	6.2	-8.2	257	0.89
	CVL-10	6.2	-8.2	262	0.78
	CVL-11	6.2	-8.2	260	0.85
	CVL-08	6.2	-8.2	281	1
	GBO-12	5.4	-7.6	167	1
	GBO-05	5.4	-7.6	151	0.88
	GBO-06	5.4	-7.6	154	0.64
	GBO-07	5.4	-7.6	176	0.43
	GBO-09	5.4	-7.6	176	0.2
	GBO-17	5.4	-7.6	160	0.84
Nigeria	OBE-83	5.3	8.5	121	1
	OBE-84	5.3	8.5	125	1

Tanzania	UDJ-01	-8.6	35.9	510	0.25
	UDJ-02	-8.6	35.9	630	0.25
	VTA-01	-7.8	37	296	0.28
	VTA-02	-7.8	36.9	583	0.52
	VTA-03	-7.8	36.9	670	0.8
	VTA-04	-7.7	36.9	608	0.6
	VTA-14	-5.1	38.7	595	0.52
	VTA-19	-7.9	36.9	610	1
	VTA-23	-7	37.8	391	0.4
	VTA-24	-7.2	37	587	0.4
	VTA-28	-6	37.7	508	0.4
	VTA-29	-6	37.7	771	0.4
	VTA-34	-5.5	38.8	91	0.4
	VTA-35	-5	38.8	198	0.4
	VTA-36	-5	38.8	288	0.2
	UDZ-03	-7.8	36.9	789	1

1015
1016

Table S7 Parameters of the cluster-specific height-diameter allometric models used in this study. A Weibull model (ref.[58]) was used.

Cluster	Sites with field height	Heights sampled	Sites without field height	a	b	c
high EA	ABE, KUK, RWE(high)	1690	MAU(high), VIR(high)	1671	0.0019	0.485
high Kilimanjaro	KIL(high)	677		25.949	0.035	1.016
dry EA	KUL, NYI	679		1314	0.0032	0.392
dry WA (& YAY)	BAB,MBA, OKU	1467	NGE, YAY	25.677	0.047	0.926
wet WA	NGI, TNP	331	BAK, NIM, RUM (low)	46.087	0.063	0.659
mid Albertine/EA	BUR,BWI(high), ITO(high), KAH, NYU, RWE(low)	5363	BON, JAB, KAF, MAU (mid), SHE, VIR(low)	30.409	0.025	1.021
low Albertine	BUD, ITO(low), KIB	617	BWI (low), MPG, RAB	99.994	0.023	0.699
Mt Cameroon	CAM	4014	RUM (mid)	28.845	0.03	0.989
mid EAM & Mozambique	KIL(low), TAI, UDZ, USA(mid)	1046	CHI, LIC, MAB, MUL, UKA(mid), ULU(mid)	127.507	0.02	0.592
low EAM	USA(low)	109	GUU, UKA(low), ULU (low)	50.042	0.025	0.96
hyper dry EA	MAR	301	HAR	25.691	0.195	0.493

EA: East Africa, WA: West Africa, EAM: Eastern Arc Mountains, low: low elevations, mid: mid elevations, high: high elevations. For site codes refer to Table S5.

Plots were clustered using selected climatic variables (mean annual temperature, temperature seasonality, total precipitation, precipitation seasonality and minimum temperature). We computed aboveground carbon estimates for sites with field height (H) measurements available, using: a) field-H, b) cluster-specific-H-model and c) all-sites-H-model. For most sites (except two) approach b (cluster-specific-H-model) outperformed approach c (all-sites-H-model), therefore, approach b was used for sites with no field measurements of height.